Derivation of a macroscopic mixture model for two-phase turbulent flows

G. Bois

Version of Record: https://www.sciencedirect.com/science/article/pii/S0017931021006037
Manuscript_1f77121c226d707bd0192535bd7312b5

Derivation of a macroscopic mixture model for two-phase turbulent flows

G. Bois[a]

[a] *Université Paris-Saclay, CEA, Service de Thermo-hydraulique et de Mécanique des Fluides (STMF), CEA Centre de Saclay, Gif-sur-Yvette, 91191, France*

Abstract

This article addresses the issue of reduced models to describe turbulent two-phase flows in industrial applications. A spatially-averaged mixture or drift-flux model is derived theoretically from the local instantaneous Navier-Stokes description. Reynolds-averaging and space-averaging are applied successively. Between these two steps, a model reduction is achieved to account for the non-equilibrium between phases *via* algebraic relations. Applications of this work are not limited to porous media but also include macroscopic descriptions to model high-shear regions developing near the walls for internal flows. Thermal effects, heat transfer at the wall and phase-change are also considered and briefly discussed. The final model describes the evolution of mixture variables, including effects of both sub-filter spatial variations, turbulence, and local non-equilibrium in velocity, pressure and enthalpy. This analysis provides bridges between different approaches to model two-phase flows (local instantaneous description, two-fluid model, local drift-flux model and spatially-averaged drift-flux model). It clarifies the content of each model involved by defining them in terms of local instantaneous quantities. Turbulent fluctuations and phase intermittency are crucial mechanisms. Important effects to model also include void fraction dispersion and turbulent diffusion; then, it is necessary to model the relative velocity, including the drift velocity orthogonal to gravity induced by the complex interactions between turbulent velocity fluctuations and the interfacial momentum transfer.

The final macroscopic (spatially-averaged) mixture formulation is open, in the sense that expressions to model the various terms representing the physics of the small scales are not provided; instead, the physical sense and

Email address: guillaume.bois@cea.fr (G. Bois)

the origin of these models are discussed. The paper is meant as a basis on which analyses on local imbalance assumptions or relative velocity closures can be assessed. CFD simulations can provide information to complement experiments in technically challenging physical conditions or on processes essential to the models yet difficult to access experimentally (such as interfacial transfers for instance). Different kinds of two-fluid models can be tested to analyse their consequences on the macroscopic spatially-averaged model. In addition, a new path to calibrate closure laws or propose new models is opened based on finer-scale descriptions. Guidelines to use fine simulations along with the open expressions to derive closure relations either for the local drift-flux or for the spatially-averaged models are presented. They concern the modelling of the local relative velocity, the spatial average of the diffusion of void fraction and of the pressure drop.

Keywords: Two-phase flow, volume averaging, homogenisation, up-scaling, two-fluid model, turbulent dispersion, effective diffusion, sub-channel modelling, drift-flux model

---

Nomenclature

Acronyms

CFD Computational Fluid Dynamics

CHF Critical Heat Flux

CMFD Computational Multi-Fluid Dynamics

DNS Direct Numerical Simulation

EOS Equation Of State

LHS Left Hand Side

PDE Partial Differential Equation

RANS Reynolds-Averaged Navier Stokes

REV Representative Elementary Volume

RHS Right Hand Side

Subscript

∇P	pressure-induced
$\Re$	viscous-induced
disp	dispersion
pd	pressure drop
f	fluid
k	k phase
l	liquid phase
M	macroscopic property (mean and volume-averaged)
m	mixture property
r	relative
v	vapour phase
w	wall
z	axial component

Greek symbols

α	void fraction
χ	phase indictor function
χ_f	indicator function of the fluid phase
δ	Dirac (delta) function
Γ_M	macroscopic vaporisation term ($\langle \Gamma_v \rangle_f$)
Γ_v	interfacial mass (evaporation) flux
κ	curvature
λ	conductivity or axial liquid pressure gradient, Eq. (23)

μ viscosity

$\mu^\star$ combination of viscosities

ϕ porosity

ρ density

σ surface tension

τ viscous stress (local)

ω curl of velocity

Latin

c_p thermal capacity at constant pressure

$\dot{m}_v$ interfacial phase-change rate

$\overline{h}_r$ enthalpy difference $\overline{h}_v^v - \overline{h}_l^l$

$\overline{p_l^b}^l$ bubble-induced pressure perturbation, Eq. (22)

$\overline{p_l^{SP}}^l$ liquid pressure in the absence of the perturbation, Eq. (22)

$\overline{p}_r$ pressure difference $\overline{p}_v^v - \overline{p}_l^l$

$\mathcal{L}^{\text{vap}}$ latent heat of vaporisation

$\mathcal{M}$ macroscopic mechanism

$\mathcal{N}$ dimensionless group

$\mathcal{T}^t$ turbulent stress

$\mathcal{T}^v$ viscous stress (mean)

$\mathcal{T}^{dr}$ diffusion stress (due to relative velocity)

Re Reynolds number

$\overline{\mathbf{u}}_D$ macroscopic drift velocity, $\overline{\mathbf{u}}_{D1} + \overline{\mathbf{u}}_{D2}$, Eq. (50)

$\overline{\mathbf{u}}_m$ barycentric velocity

$\overline{\mathbf{u}}_r$ relative velocity

$\overline{\mathbf{u}}_{v\to m}$ drift or diffusion velocity

$\mathbf{n}_v$ interface normal (towards liquid)

$\mathbf{u}$ velocity

$\mathbf{x}$ local position vector (x, y, z)

$\mathbf{D}^r$ macroscopic diffusion tensor $(\langle \mathcal{T}^{dr} \rangle_f)$

$\mathbf{D}_M$ macroscopic dispersion, Eq. (47)

$\mathbf{e}$ unit vector

$\mathbf{I}$ identity tensor

$\mathbf{M_k^{RANS}}$ momentum interfacial transfer into phase k from the other phase $(\mathbf{M_v^{RANS}} + \mathbf{M_l^{RANS}} = 0)$

$\mathbf{M_M}$ mixture momentum source $(\langle \mathbf{M_m} \rangle_f)$

$\mathbf{M}_k$ interfacial transfer into phase k

$\mathbf{M}_m$ mixture momentum source

$\mathbf{Q}$ heat flux

$\mathbf{Q}^c$ correlation heat flux, Eq. (33)

$\mathbf{Q}^f$ conduction heat flux, Eq. (37)

$\mathbf{S_M}$ deviatoric part of the macroscopic stress tensor, Eq. (54)

$\mathbf{T}$ macroscopic turbulent tensor $(\langle \mathcal{T}^t \rangle_f)$

$\mathbf{V}$ macroscopic viscous tensor $(\langle \mathcal{T}^v \rangle_f)$

$\widetilde{p_l}$ reference pressure

c vapour mass fraction

C_D	drag coefficient
d_b	bubble mean diameter
D_h	hydraulic diameter
e	channel width
g	gravitational acceleration
h	enthalpy
K	closure parameters (K_D, K_L and K_{Disp} for the drag, lift and dispersion respectively)
K_M	tensor set of coefficients to model $\mathbf{T}$, Eq.(53)
l_ξ	microscopic scale of variation of the variable ξ
$L_{\langle\xi\rangle}$	macroscopic scale of variation of the filtered variable $\langle\xi\rangle$
p	pressure
$p^\star$	dynamic pressure
r	radial coordinate
r_0	characteristic lengthscale of the filter kernel
T	temperature
t	time
V	averaging volume
y	wall-normal coordinate
z	axial coordinate

Mathematical symbols

$\delta\phi$	deviation of ϕ from the Favre filtering $\widetilde{\phi}$
$\delta_s\phi$	deviation of ϕ from the volume average $\langle\phi\rangle_f$

$\widetilde{\phi}$	Favre averaging (fluid- and density-weighted filtering) of quantity ϕ, Eq. (43a)
$\overline{\phi}^k$	phase average of ϕ
$\overline{\phi}$	statistical average of ϕ
$[\![\ ]\!]$	interfacial jump (liquid/vapour difference)
$\langle\ \rangle_f$	weighted volume average
$\langle\ \rangle$	volume average or space filter
$\mathcal{D}_{\mathbf{u}}$	One-fluid local viscous operator
$\nabla^\dagger$	sum of the gradient and its transpose ($\nabla + \nabla^T$)
$\nabla_\phi \cdot$	divergence weighted by porosity ($\nabla_\phi \cdot \zeta = \frac{1}{\phi}\nabla \cdot (\phi\zeta)$)
$\nabla_s \cdot$	surface divergence
$\|\mathbf{v}\|$	norm of $\mathbf{v}$
ϕ'	fluctuation of ϕ with respect to the phase average
D/Dt	material or substantial derivative
Superscript	
$\dagger$	sum of a second-order matrix and its transpose
sat	saturation property
mod	model
ref	reference
extra	Reynolds stresses of the dispersed phase
AM	added mass
c	cross-correlation
D	drag

i	interfacial
L	lift
LD	laminar dispersion
SP	single phase
t	turbulent
TD	turbulent dispersion

1. Introduction

Many industrial applications involve complex two-phase flows for transport, chemical reactors or heat exchangers. They are central to the development of the oil and gas or nuclear industries. These flows are very strongly dominated by interfacial transfers; interfacial forces or heat and mass transfers have to be characterised and modelled. A particular concern of the nuclear industry is the presence of bubbles at the wall where boiling characteristics strongly depend on the distribution and trajectories of bubbles. Hence, the prediction of local and time-averaged void fraction is a major issue determinant in safety analysis and to know the conditions of Critical Heat Flux (CHF) occurrence.

The physical behaviour of two-phase bubbly flows is strongly related to local phenomena occurring in the surroundings of bubbles or interfaces (an increase of the dissipation close to the interfaces, boundary layer growth and detachment, wake's structure and interactions). Classical experiments struggle to clearly isolate the individual role of each of these phenomena. A detailed description of all the interfaces and the associated transfers is out-of-reach for most of industrial applications. Thus, two-fluid models [1, 2, 3] have been developed to assess and predict this local distribution of void fraction. To this end, they rely in particular on interfacial force models to build a two-fluid Euler-Euler description of the Reynolds-Averaged Navier-Stokes (RANS) equations where the evolution of each phase is described separately by a set of conservation equations. Conservation principles lead to an underdetermined set of equations and additional local relations are necessary to achieve a determined set; they are usually inferred from experimental measurements [see *e. g.,* 4, for the determination of the drag force]. Because of the strong dominance of buoyancy and strong convection in industrial

applications, most efforts were focused on the accuracy of one-dimensional closures, and the precise modelling of void fraction distribution in the cross-flow plane due to other interactions still lags behind, with a lower accuracy and more difficulties to provide generally applicable relations. Liu et al. [5] propose a generic framework for multi-field two-phase flow based on the two-fluid model for applications to any flow regime by the consideration of several fields within each phase.

In the end, even this local two-fluid approach gets expensive to accurately capture boundary layers and the effect of complex geometries. Hence, in order to further reduce the computational cost and enable extensive parametric studies that are required in industrial applications (for instance for design, operation or safety analysis), coarser models have been developed. They rely on averaging techniques to incorporate the effect of (time-averaged) local gradients. The development of models based on homogenisation techniques is an essential feature of the description of flows in porous media [6] with applications to soil science or petroleum engineering and many other fields. Macro-scale modelling[1] has been very active in this community. In many of the applications to fluid flows in porous media, Darcy's law is used as an approximate momentum equation for each phase [7, 8]; Darcy-Forchheimer model has also been used to obtain a macro-scale description of turbulence in porous media [9]. Capillary effects and contact line motion are also often dominant features of the flow considered. For instance, Gray et al. [10] provide guidelines for closure relations based on a constraint to the energy of the system derived from the second law of thermodynamics. Jackson et al. [7] derive averaged models satisfying similar thermodynamic constraints.

In this paper guided by nuclear applications, flows with very high Reynolds numbers are considered. Macroscopic models (*i. e.,* obtained by spatial averaging) for turbulent flows were initiated for nuclear applications though it was mostly applied to the macroscopic description of fuel assemblies where the exact description of wall structures become prohibitively expensive; this methodology leads to models referred to as sub-channel or component models and codes. Several works [1, 2, 11, 12, 13, 14, 15, 16, 17] present a specific derivation for targeted applications with appropriate simplifications. Most often, drastic simplifications lead to one-dimensional models fully-averaged

[1]In this paper, the terminology *macro-scale* or *macroscopic* refers to spatial averaging or homogenised description.

over the cross-sectional area, associated with empirical closure relations. To the best of our knowledge, the homogenised equations for the general three-dimensional case are not derived from local principles, yet the cross-sectional distribution of velocity and void fraction shows significant variations in geometry such as tube bundles or flat rectangular channels. The complete 3D description of the partially-averaged system is then necessary.

In parallel to the distinction between the local and macroscopic approaches that comes from resorting to a space-averaging operator, another key differentiating feature between the models is the consideration of the two phases either as a mixture or as separate entities. When the mixture balance equations are considered, different models can be derived depending on the assumption of equilibrium or non-equilibrium between the phases for the velocity, the enthalpy and the pressure. When total equilibrium is assumed, the homogeneous equilibrium model is obtained. Alternately, non-equilibria can be considered either by additional transport equations or by algebraic closures. When an algebraic closure for the relative velocity introduces mechanical non-equilibrium [see *e. g.,* 18, 19, for the application of the homogenised drift-flux to gas-liquid flows in vertical or horizontal pipes], the drift-flux model [20] is obtained as a simpler formulation in comparison to the more complete two-fluid formulation. Most modelling efforts were carried in one dimension (with the notable exception [21]). Consequently, generalisation of the drift-flux model's closures to multi-dimensional flows and geometries is not straightforward. Besides, in practical applications, it is used in conjunction with area-averaging. Here, we will be interested by the local three-dimensional description of the drift-flux model as an intermediate step.

The drift-flux model can only be used with dedicated closure relations, sometimes based on local considerations and principles [as in *e. g.,* 22, for the modelling of the cross-section averaged void fraction accounting for both the distribution of concentration across the duct and the effect of local relative velocity between the two-phases] or on fully empirical correlations. However, these approaches do not naturally integrate all the principles embedded in the local conservation laws. As a consequence, the closure relations provided may not satisfy them all locally. On the contrary, the methodology proposed here relies on local solutions that satisfy these local governing equations and henceforth ensures that they are preserved at the macroscopic scale; we utilise conservation laws and governing equations on local phase quantities to provide constraints to mixture and spatially-homogenised quantities. Therein,

the approach used here is, in essence, fundamentally different from works of for instance [18, 22] or subsequent efforts that *assume* local distributions of void fraction or velocity to derive correlations for mean flow description. It is also very different for example from the work of [4] on the drag force closure, which derives correlations for the drag coefficient and relative velocity from partial observations of local fields, independently of conservation principles.

To the best of our knowledge, rigorous derivations of macroscopic models have been applied mostly to single-phase applications [23, 24, 25, 26, 27, 28, 29, 30]. Some works were also dedicated to the accurate description of the transition between the porous region and the flow in a free region [31, 32, 33]. Another example provided by the work of Soulaine and Quintard [9] focused on the effect of the microscopic structure of the porous media on the macro-scale description of turbulence, with the prospect of deriving for instance an apparent permeability tensor. We can also cite the contribution of Clavier et al. [34] focused on the modelling of friction closure laws in inertial multi-phase flows or a review by Wang et al. [35] on meso-scale drag modelling that reveal very different methodologies for deriving averaged models.

There are two essential differences of the approach proposed here. First, the methodology is applied to two-phase turbulent flows, where turbulent fluctuations and phase intermittency are crucial. The second major difference is that the filtering and homogenisation proposed here can be applied in free regions of the flow and not necessarily to porous regions where the goal is to eliminate the need for the description of the actual solid structure topology and to replace it by modelled sources. Indeed, our objective is to describe the flow at the macroscopic scale (*i. e.,* to capture only the gradients of spatially averaged fields) and to account for high-shear regions indirectly by means of models. Applying this methodology to multiphase flows increases the complexity.

In this article, a two-step up-scaling strategy from the local instantaneous description to the macroscopic (sub-channel) model is presented. In brief, the intent is to provide a sound and coherent basis for the up-scaling in which the various macroscopic models will consistently depend on the underlying local fields. To the best of our knowledge, we derive a local equation governing the relative velocity (equation (16)) that is not available in the literature; our derivation enables both (i) a better understanding of the diverse effects competing to govern the void fraction distribution, in particular in the cross-sectional direction, and (ii) the clear connection between the two-fluid and the drift-flux models at the local scale. Various degrees of simplification of

this equation are possible to build intermediate models. When reduced to an instantaneous local closure, this Partial Differential Equation (PDE) becomes algebraic and it completes the description of a local three-dimensional drift-flux model.

The paper is organised around the various scales and simplifications considered. Section 2 describes the steps taken to reach the macroscopic description from the local instantaneous balance. Along with definitions of the different approaches, it gives the objectives of the procedure based on fine-scale models and simulations, and it exposes the scope of application.

The first up-scaling step is very classical and leads to the widely-used Euler-Euler two-fluid model. It is based on the local instantaneous governing equations describing two-phase flows introduced in section 3; this step leads to the two-fluid model presented in section 4 and some important issues relative to its closure are discussed. In particular, we have selected the proposal of du Cluzeau et al. [36] for interfacial transfers because it involves fewer assumptions regarding local non-equilibrium of pressure and interfacial momentum transfer compared to the more classical one-pressure two-fluid approaches. This distinction is important because its effect remains visible at the end of the second up-scaling step.

Then, the second up-scaling step involves a space averaging of the RANS two-fluid model. But instead of a direct application of the spatial filter to the two-fluid model, we are interested in this work in the homogenisation of a simpler local drift-flux model. Thus, the two-fluid model with two separate sets of equations is simplified into a drift-flux model in section 5. The second up-scaling step (space-averaging) is then applied to this simplified system to lead to the set of equations governing the macroscopic description of the mixture as used in sub-channel codes (section 6).

Lastly, section 7 gives some insights into various possibilities offered by the present derivation; it details the procedure to apply in order to inform macroscopic models. We show how the equation derived for the local relative velocity can be simplified to various degrees to develop intermediate models between the local two-fluid and a local drift-flux model. We also illustrate how to apply the up-scaling methodology on two important mechanisms for industrial applications, namely the void fraction dispersion and the macroscopic pressure drop. Finally, section 8 draws the main conclusions of this work and presents prospects in terms of validation and model developments based on this up-scaling methodology.

2. Scope and objectives

This section presents the up-scaling strategy as illustrated on figure 1. Two important aspects define each system: (i) the consideration of the *fluid system* and (ii) the temporal and spatial scale examined. From these elements, the local instantaneous description of the two-fluid system is given by governing balance equations and interfacial jump conditions. Statistical averaging generates the local two-fluid system from which the local drift-flux model can be obtained by reduction of the number of variables (via algebraic expressions for the non-equilibria between phases). Lastly, the macroscopic scale is achieved by volume-averaging the local drift-flux model.

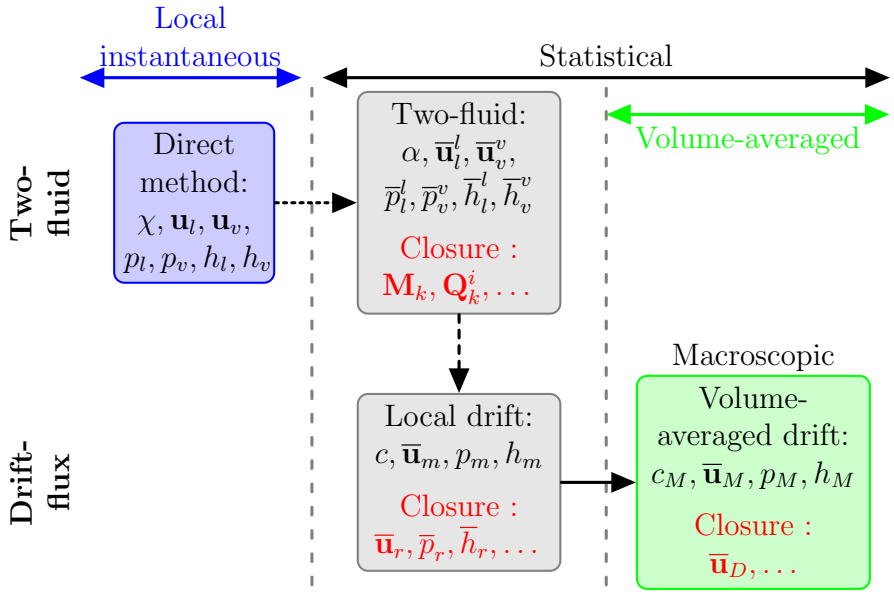

Figure 1: Up-scaling description with the *scales* considered, the fluid-*system* and the operations connecting them. Definitions of *scales*: local instantaneous, statistical and macroscopic (both statistical and volume-averaged). Consideration of the two-phase *system*: two-fluid or drift-flux. Connecting mechanisms: statistical averaging (dotted horizontal arrow), volume averaging (continuous horizontal arrow), model reduction (dashed vertical arrow).

This derivation aims to fully describe the theoretical content of the macroscopic models and express it in terms of local instantaneous flow description. Then, we will analyse this content with reference simulations.

Obviously, developping closure relations from numerical simulations performed by the two-fluid model requires careful validation of it; in particular, it is essential that the model, considered as a reference, be capable of accurate predictions of the local mechanisms involved such as cross-flow void fraction distribution. Indeed, in this up-scaling analysis of numerical simulations, the closures' derivation relies on the averaging of microscopic correlations (of velocities, etc.) and forces. Besides, because of the paramount importance of the interfacial transfers at the local scale and their influence on the determination of the local void fraction distribution, our efforts in the derivation of the two-fluid model are attentive to the recent progress in the modelling of these transfers and of the corresponding pressure non-equilibrium. We believe that these elements are essential to correctly model the mechanisms in the cross-flow direction and should be considered properly during the model reduction and homogenisation.

In other words, we need to have a reliable two-fluid model to produce reference data that captures relevant local physical phenomena. In order to take the maximum advantage of the local model capabilities, it is necessary to have explicit relations between the various scales considered, even if the macroscopic system obtained is under-determined and will require additional closures; it will then be the specific purpose of dedicated CFD studies to propose and assess these closure relations, with the support of experimental data. The basic idea behind our approach is to take advantage of the resolution of local fields provided by the two-fluid model to inform averaged models by the derivation of closure relations either for a local drift-flux model or for a spatially-averaged macroscopic description.

Thus, the complex requirements to transform the under-determined system into a determined one, called closure relations, can be interpreted in terms of local quantities (as shall be seen in section 6) and therefore, it will be easier to model them in two parts (one from the closure of the two-fluid model itself and the other provided by the variations of the local two-fluid variables), separated in between by the two-fluid numerical resolution (see Figure 1). This intermediate resolution requires a validated model but ensures the consistency of the solution with basic principles, whilst granting access to secondary quantities (*i. e.,* additional variables that are not the main unknown transported and solved in the system) in a more consistent and accurate way. Some of these secondary variables are useful to provide reference information to be integrated into a macroscopic model. Indeed, we shall see that, in the process, it will be necessary to access the local variations of com-

plex quantities (such as interfacial transfers for instance), which cannot be observed directly on experiments. This new approach, usually referred to as *up-scaling methodology*, relies on so-called *numerical experiments*. It has recently become a plausible alternative to the historical model derivation with the increasing capabilities of Computational Multi-Fluid Dynamics (CMFD) because numerical solutions to the local two-fluid model can be produced in relevant conditions and for a broad range of physical conditions.

Finally, our intent is to progress in modelling the evolution of macroscopic variables in two- or three-dimensions. The purpose of the macroscopic model is to comprehend the effect of the geometry on the complex macroscopic flow reorganisation. In this way, this model aims at applying the essence of the two-fluid model to larger geometries to extend its applications. Macroscopic models are also perfectly suitable for parametric studies in design or safety analyses to reduce the computational cost. By clarifying the intermediate steps and assumptions, we expect to provide a better understanding of the complex evolution of the relative velocity and void-fraction distribution in the three-dimensional case.

3. Local instantaneous governing equations

This section introduces the local variables, the conservation equations and the interfacial jump conditions. The reader familiar with this description can go to section 4. We consider a liquid-vapour flow, with phase-change occurring at discontinuous interfaces. The formulation relies on the classical basis for Direct Numerical Simulations (DNS), namely the one-fluid Navier-Stokes equations [37, 38], given by

$$\frac{\partial \chi_v}{\partial t} + \mathbf{u}^i \cdot \nabla \chi_v = 0, \tag{1a}$$

$$\frac{\partial \rho}{\partial t} + \nabla \cdot (\rho \mathbf{u}) = 0, \tag{1b}$$

$$\frac{\partial \rho \mathbf{u}}{\partial t} + \nabla \cdot (\rho \mathbf{u}\,\mathbf{u}) = -\nabla p + \rho \mathbf{g} + \mathcal{D}_{\mathbf{u}} + \sigma \kappa \mathbf{n}_v \delta^i, \tag{1c}$$

$$\frac{\partial \rho\, h}{\partial t} + \nabla \cdot (\rho \mathbf{u} h) = \nabla \cdot (\lambda \nabla T) + \frac{\partial p}{\partial t} + \nabla \cdot (p\mathbf{u}) - \left[\!\!\left[\frac{p}{\rho} \right]\!\!\right] \dot{m}_v \delta^i \tag{1d}$$

where each of the one-fluid variables is defined as a mixture of phase variables: $\psi = \sum_k \chi_k \psi_k$ (ψ can be $\mathbf{u}$, p, h, T, ρ, μ or λ, respectively the velocity,

pressure, enthalpy, temperature, density, dynamic viscosity or conductivity) and the notation $[\![\,]\!]$ refers to the jump through the interface defined as $[\![1/\rho]\!] = 1/\rho_l - 1/\rho_v$. The main variables of the local description are illustrated on figure 2. The subscript k refers to the phase (either l for liquid or v for vapour). Physical properties are assumed constant within each phase. Both phases are considered incompressible. $\mathbf{g}$ is the gravity vector, σ is the surface tension. δ^i is a three-dimensional Dirac impulse at the interface i. $\kappa = -\nabla_s \cdot \mathbf{n}_v$ is twice the mean curvature (usually negative for bubbles) defined from the surface divergence $(\nabla_s \cdot)$ of the unit normal to the interface $\mathbf{n}_v$, oriented towards the liquid. The normal vector is related to the phase indicator function χ_v by $\nabla\chi_v = -\mathbf{n}_v\delta^i$ where χ_v is equal to one in the vapour and zero in the liquid. This phase indicator function is transported in equation (1a) by the interfacial velocity $\mathbf{u}^i$ defined from the phase velocities $\mathbf{u}_k$ at the interface vicinity as:

$$\mathbf{u}^i = \mathbf{u}_k - \frac{\dot{m}_k}{\rho_k}\mathbf{n}_k \tag{2}$$

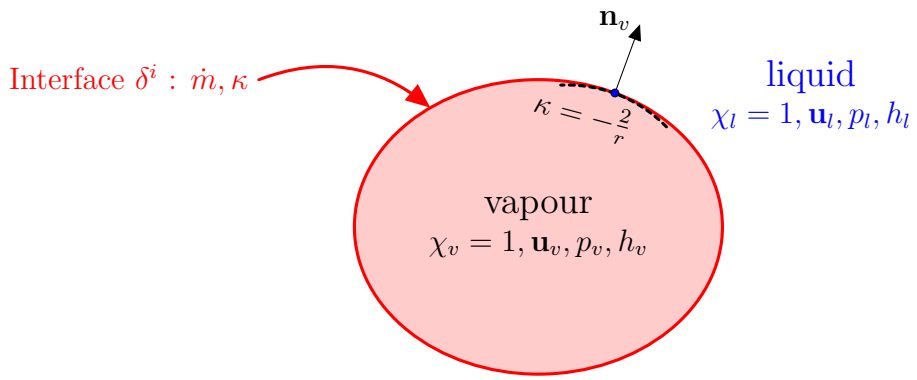

Figure 2: Definition of local variables.

This equation is valid on both sides of the interface thanks to the jump conditions at the interface [14, 39, 40, 41, 42].

The last term in the RHS of equation (1c) ensures that the momentum equation implicitly contains the correct stress boundary condition at the interface. The diffusion term $\mathcal{D}_\mathbf{u}$ is defined by

$$\mathcal{D}_\mathbf{u} = \nabla \cdot \left[\mu \left(\nabla^\dagger \mathbf{u} + 2\dot{m}_v \left[\!\left[1/\rho\right]\!\right] \mathbf{n}_v\, \mathbf{n}_v \delta^i\right)\right] \tag{3}$$

where $\nabla^\dagger = \nabla + \nabla^T$ is the sum of the gradient and its transpose. As we consider incompressible phases with constant viscosity, the diffusive effect of $\nabla^T \mathbf{u}$ is limited to an interfacial contribution. The last term of equation (3) finds its origin in the velocity jump due to phase change. It has to be considered accurately to avoid the appearance of non-physical pressures at the interface.

Similarly, the last term in the energy balance (1d) appears to compensate for the interfacial dirac generated by $\nabla \cdot (p\mathbf{u})$ (this divergence includes a dirac delta function because p and $\mathbf{u}$ are two Heaviside functions). Energy production by viscous and gravitational forces is neglected in the balance of enthalpy by comparison to heat transfers. The interfacial phase-change rate $\dot{m}_k$ is related to velocities at the interface by:

$$\dot{m}_k = \rho_k(\mathbf{u}_k^i - \mathbf{u}^i) \cdot \mathbf{n}_k^i \tag{4}$$

The equation system (1) and the subsequent definitions describe the local and instantaneous evolution of the two-phase system. It allows to determine the evolution of the vapour phase indicator function χ_v, the interfacial phase-change rate $\dot{m}_v$, and the one-fluid velocity $\mathbf{u}$, pressure p and enthalpy h. Its direct resolution requires very fine spatial and temporal discretisations to enable the resolution of the broad range of scales involved. In order to have a determined system, it is important to provide a relation to determine the temperature from the enthalpy and pressure ($T = T(h, p)$) and a constraint to the interfacial temperature T^i (for instance, equality to the saturation temperature $T^i = T^{\text{sat}}$ reflecting local thermodynamic equilibrium of chemical potential). It enables the determination of the phase-change rate at the interface from the jump in heat flux: $[\![\lambda \nabla T]\!] \cdot \mathbf{n}_v = \dot{m}_v [\![h^{\text{sat}}]\!]$. This interfacial jump is naturally included in the one-fluid formulation of equation (1d) ([37, Eq. (39)] or [41]).

4. Statistical averaging: the RANS Euler-Euler two-fluid model

Based on the local description of conservation equations for each phase and jump conditions at the interface [37] summarised in the previous section, two-fluid models can be established by application of a statistical averaging operator. An intense and thorough work on closure development is then required to achieve a set of equations that can be used in industrial applications [2, 3]. In the following section (section 4.1), a focus on momentum conservation in each phase is presented. Then, section 4.2 introduces an alternative

(but equivalent) description of the two-fluid model based on relative and mixture velocities. This formulation clearly shows the connections between the two-fluid model and the drift-flux model derived in section 5.2. In section 4.4, connections between forces (or more generally closure relations) and the relative velocity are discussed in view of modelling possibilities. Lastly, the global two-fluid system is completed in section 4.5 by the mass and energy conservation equations.

4.1. Statistical average of phase momentum equations

For any quantity ψ, we define a statistical average $\overline{\psi}$ with the classical properties of a Reynolds averaging operator. Phase-averaging is obtained by weighting this average by the phase-indicator function $\overline{\psi_k}^k = \overline{\chi_k \psi_k}/\overline{\chi_k}$. The average of the vapour indicator function is called the void fraction $\alpha = \alpha_v = \overline{\chi_v}$. Then, the decomposition into time-averaged and fluctuating quantities is performed with respect to the phase-averaging operator; for instance, the velocity $\mathbf{u_k}$ is split into mean and fluctuating parts $\mathbf{u_k} = \overline{\mathbf{u_k}}^k + \mathbf{u'_k}$. Applying the statistical average to the Navier-Stokes equations written separately for each phase and using the jump conditions at the interface, one gets [2, 36]

$$\frac{D\left(\alpha_k \rho_k \overline{\mathbf{u_k}}^k\right)}{Dt} = -\nabla\left[\alpha_k\left(\overline{p_k}^k - \widetilde{p_l}\right)\right] + \alpha_k \rho_k \mathbf{g} + \nabla \cdot \left(\mathcal{T}_k^v - \alpha_k \rho_k \overline{\mathbf{u'_k} \mathbf{u'_k}}^k\right) + \mathbf{M_k}$$
$$\text{with} \quad k \in [l, v] \quad \text{and} \quad \mathbf{M_l} + \mathbf{M_v} = \overline{\sigma \kappa \nabla \chi_v} \tag{5}$$

where $D\left(\alpha_k \rho_k \overline{\mathbf{u_k}}^k\right)/Dt = \partial\left(\alpha_k \rho_k \overline{\mathbf{u_k}}^k\right)/\partial t + \nabla \cdot \left(\alpha_k \rho_k \overline{\mathbf{u_k}}^k \overline{\mathbf{u_k}}^k\right)$ is the material or substantial derivative. The interfacial transfer $\mathbf{M_k}$ is defined by $\mathbf{M_k} = \overline{(\dot{m}_k \mathbf{u_k} \mathbf{n_k} + p_k \mathbf{I} - \mu_k \nabla^\dagger \mathbf{u}_k) \cdot \nabla \chi_k}$ with $\mathbf{I}$ the identity tensor. Indices l and v are respectively related to liquid and gas phases. The sum of hydrostatic and dynamic pressures p is defined relatively to an arbitrary reference pressure $\widetilde{p_l}$ (constant). It is worth mentioning that the condition of adherence applied to the local instantaneous velocity fields (classical in continuum mechanics) remains verified after the statistical average and leads to a nil phase-averaged velocity at the wall for both phases. $\mathcal{T}_k^v$ is the mean viscous stress defined as $\mathcal{T}_k^v = \overline{\chi_k \mu_k \nabla^\dagger \mathbf{u_k}} = \alpha_k \overline{\tau_k}^k$ with $\tau_k = \mu_k \nabla^\dagger \mathbf{u_k}$. However, for accuracy and completeness, it is important to stress that $\overline{\tau_k}^k$ cannot be expressed fully in terms of averaged variables (α_k and $\overline{\mathbf{u}}_k^k$) due to the non-commutativity of the phase-averaging operator with space derivatives

($\overline{\nabla \mathbf{u_k}}^k \neq \nabla \overline{\mathbf{u}}_k^k$). As a consequence, we have :

$$\mathcal{T}_k^v = \overline{\chi_k \mu_k \nabla^\dagger \mathbf{u_k}} = \alpha_k \overline{\tau_k}^k = \alpha_k \mu_k \nabla^\dagger \overline{\mathbf{u}}_k^k + \mu_k \left(\overline{\mathbf{u}}_k^k \nabla \alpha_k - \overline{\mathbf{u_k} \nabla \chi_k} \right)^\dagger \quad (6)$$

This expression reveals that the closed equivalent to the mean viscous stress $\breve{\tau}_k = \alpha_k \mu_k \nabla^\dagger \overline{\mathbf{u}}_k^k$ must be completed by the symmetric viscous effect of the cross correlation $\left(\overline{\mathbf{u}}_k^k \nabla \alpha_k - \overline{\mathbf{u_k} \nabla \chi_k} \right)^\dagger$ between fluctuations at the interface of phase velocities and interface orientation. This closure issue is overlooked in most descriptions of the two-fluid model [1, 2, 3] and it will be neglected without physical justification here; in theory, a magnitude assessment or an appropriate modelling of this term would be required. $\mathcal{T}_k^t = \alpha_k \rho_k \overline{\mathbf{u'_k} \mathbf{u'_k}}^k$ is the turbulent stress in phase k. $\mathbf{M_m} = \overline{\sigma \kappa \nabla \chi_v}$ is the mixture momentum source due to surface tension effects [2, p. 99]. In the terminology of this article, we distinguish the *interfacial* transfer $\mathbf{M_k}$ that goes from the interface to phase k, from the *inter-phase* transfer $\mathbf{M_k^{RANS}}$ (defined below by equation (8)) that goes from the other phase into phase k.

The pressure term is classically written as a pressure gradient whereas the remaining part $(\overline{p_k}^k - \widetilde{p}_l)\nabla \alpha_k$ is introduced into the inter-phase momentum transfer $\mathbf{M_k^{RANS}}$ along with the interfacial transfer $\mathbf{M_k}$. The pressure gradient considered is relative to the sub-part $\overline{p_l^{SP}}^l$ of the true liquid pressure, considered in the absence of the perturbation induced by the bubbles $\overline{p_l^b}^l$ [36].

Then, with the pressure decomposition $\overline{p}_l^l = \overline{p_l^{SP}}^l + \overline{p_l^b}^l$, the averaged Navier-Stokes equations are written in the Euler-Euler RANS formalism as

$$\frac{\partial \alpha_v \rho_v \overline{\mathbf{u_v}}^v}{\partial t} + \nabla \cdot (\alpha_v \rho_v \overline{\mathbf{u_v}}^v \overline{\mathbf{u_v}}^v) = -\alpha_v \nabla \overline{p_l^{SP}}^l - \nabla \cdot \left(\mathcal{T}_v^t - \mathcal{T}_v^v \right) + \alpha_v \rho_v \mathbf{g} + \mathbf{M_v^{RANS}} \quad (7a)$$

$$\frac{\partial \alpha_l \rho_l \overline{\mathbf{u_l}}^l}{\partial t} + \nabla \cdot \left(\alpha_l \rho_l \overline{\mathbf{u_l}}^l \overline{\mathbf{u_l}}^l \right) = -\alpha_l \nabla \overline{p_l^{SP}}^l - \nabla \cdot \left(\mathcal{T}_l^t - \mathcal{T}_l^v \right) + \alpha_l \rho_l \mathbf{g} + \mathbf{M_l^{RANS}} \quad (7b)$$

$$\mathbf{M_l^{RANS}} = -\mathbf{M_v^{RANS}} + \overline{\sigma \kappa \nabla \chi_v} - \nabla \left[\alpha_v \left(\overline{p}_v^v - \overline{p}_l^l \right) \right] - \nabla \overline{p_l^b}^l \quad (7c)$$

where relations between interfacial $\mathbf{M_k}$ and inter-phase $\mathbf{M_k^{RANS}}$ transfers are given by du Cluzeau et al. [36] as:

$$\mathbf{M_v^{RANS}} = \mathbf{M_v} - \alpha_v \nabla \overline{p_l^b}^l - \left(\overline{p}_l^l - \widetilde{p}_l \right) \nabla \alpha_v - \nabla \left[\alpha_v \left(\overline{p}_v^v - \overline{p}_l^l \right) \right] \quad (8a)$$

$$\mathbf{M_l^{RANS}} = \mathbf{M_l} - \alpha_l \nabla \overline{p_l^b}^l + \left(\overline{p}_l^l - \widetilde{p}_l \right) \nabla \alpha_v \quad (8b)$$

Equations (8a) and (8b) define the inter-phase transfers $\mathbf{M_k^{RANS}}$ from the interfacial transfers $\mathbf{M_k}$ and the pressure contributions. Because interfaces accumulate momentum in the mixture momentum source $\mathbf{M_m}$ by means of surface tension, these transfers are different. The *inter-phase* transfers satisfy by definition $\mathbf{M_l^{RANS}} + \mathbf{M_v^{RANS}} = 0$, whereas for the *interfacial* transfers we have : $\mathbf{M_l} + \mathbf{M_v} = \mathbf{M_m}$.

Hydrodynamic constitutive relations for interfacial transfer are discussed for instance in [2, Chap. 12]. For dispersed two-phase flows, the inter-phase momentum transfer on the gas phase $\mathbf{M_v^{RANS}}$ is classically modelled as the sum of various forces (drag, lift, added mass, turbulent dispersion and wall lubrication forces). Depending on the mechanisms considered as important, other forces can be considered such as the Basset force, the virtual mass, a bubble collision force, the bubble dispersion force [43], the wall lubrication force [44, 45], etc. For more complex flow regimes such as churn-turbulent flows, extensions are available mostly for the drag force [2, Chap. 12, p. 345]. For separate phases as in annular flows, models for interfacial friction are usually considered. In the following of this section, the discussion is limited to the dispersed bubbly-flow regime. In du Cluzeau et al. [36], the authors recently suggested deep modifications to this simplified viewpoint inherited from the particle approach. Classical closures can be used as an example to illustrate the methodology but in the following, we will also emphasise the consequences of these differences and express the potential gain in modelling capacities that can derive from a richer local description. In the standard approach, the simplifications provided by the assumption of a negligible mixture momentum ($\mathbf{M_m} = 0$) and by the pressure equilibrium hypothesis ($p = \overline{p}_l^l = \overline{p}_v^v = \overline{p_l^{SP}}^l$ and $\overline{p_l^b}^l = 0$) lead to the following simplified transfer

$$\mathbf{M_v^{RANS}} = -\mathbf{M_l^{RANS}} = \mathbf{M^D} + \mathbf{M^{AM}} + \mathbf{M^L} + \mathbf{M^{TD}} \tag{9}$$

where $\mathbf{M^D}$, $\mathbf{M^{AM}}$, $\mathbf{M^L}$ and $\mathbf{M^{TD}}$ refer to drag, added-mass, lift and turbulent dispersion respectively. Closures can be provided by classical correlations as discussed in Ishii and Hibiki [2] or by Mimouni et al. [46], Neptune_CFD Development Team [47].

For a more complete description of the local physical mechanisms, the momentum transfer can be expressed as a series of forces as proposed in

du Cluzeau et al. [36]:

$$\mathbf{M_v^{RANS}} = \mathbf{M^D} + \mathbf{M^{AM}} + \mathbf{M^{TD}} + \mathbf{M^{extra}} + \mathbf{M_{\Re}^L} + \mathbf{M_{\nabla P}^L} + \mathbf{M^{LD}}, \tag{10a}$$

$$\mathbf{M_l^{RANS}} = -\mathbf{M^D} - \mathbf{M^{AM}} - \mathbf{M^{TD}} - \mathbf{M^{extra}} - \mathbf{M_{\Re}^L} + \frac{\alpha_l}{\alpha_v}\left(\mathbf{M_{\nabla P}^L} + \mathbf{M^{LD}}\right). \tag{10b}$$

$\mathbf{M_{\Re}^L}$ and $\mathbf{M_{\nabla P}^L}$ are lift induced effects produced respectively by the viscous stress and the pressure. The pressure part $\mathbf{M_{\nabla P}^L}$ does not apply symmetrically to both phases due to surface tension. In addition to classical drag, added-mass and turbulent dispersion forces, two supplementary forces are considered. The first one $\mathbf{M^{extra}} = \nabla\cdot\left(\alpha_v\rho_v\overline{\mathbf{u_v'}\mathbf{u_v'}}^v\right)$ is related to the Reynolds stresses of the dispersed phase. The second one $\mathbf{M^{LD}}$ is a dispersion force introduced and modelled in du Cluzeau et al. [48]. In practice in the classical Euler-Euler framework, the hypothesis $\mathbf{M_v^{RANS}} = -\mathbf{M_l^{RANS}}$ is always assumed and the impact of the laminar dispersion $\mathbf{M^{LD}}$ and of the additional term $\mathbf{M^{extra}}$ related to velocity fluctuations in the gas phase is neglected.

It is important to stress that $\mathbf{M_v^{RANS}}$ and $\mathbf{M_l^{RANS}}$ are not the total interfacial forces applied to each phase, but only the momentum transferred from the other phase. Thus, interfacial tension and pressure differences are excluded from it. Concerning the effect of surface tension, an important point demonstrated in du Cluzeau et al. [36] is that the local imbalance of interfacial forces do not vanish locally, even after statistical averaging. This is because of interfaces' deformations (even for small almost spherical bubbles) and their consequences on the pressure fields are not randomly distributed. In addition to inter-phase transfers, a careful consideration of the different pressures involved in the system is important for the subsequent developments. It will be important to connect them properly to the mixture pressure before the second up-scaling step involving space-averaging. Consequently, these considerations have an impact on the connections between the local two-fluid solution and the exact definitions of diffusive terms in the final homogenised description. Equations (7a) and (7b) are written in the Euler-Euler RANS two-fluid one pressure formalism (with a liquid pressure gradient also in the gas momentum equation). In the RANS Euler-Euler approach, the liquid pressure in the absence of bubbles $\overline{p_l^{SP}}^l$ is included in the resolution of the system as a main variable whereas the pressure inside the bubbles $\overline{p}_v^v$ and the liquid pressure induced by bubbles through surface tension effects have to be closed. The interpretation of the resolved pressure in a classical RANS

Euler-Euler calculation is thus tricky. The part of pressure due to surface tension $\overline{p_l^b}^l$ has an impact on the balance equation of forces (mainly in the lift force). Thus, this part which is not directly solved is considered through interfacial forces.

Here, we begin to see that an improved or richer two-fluid model involving several (and different) pressures (for instance by means of algebraic closures as initiated in du Cluzeau et al. [36] and du Cluzeau et al. [48]) will lead to a more complex mixture pressure gradient; in turn, this will create additional diffusion in the macroscopic mixture model. It will not only be due to the consideration of the mixture momentum $\mathbf{M_m}$ but it will be strengthened by the pressure imbalance $\overline{p}_l^l - \overline{p}_v^v$ and by the surface-tension-induced pressure $\overline{p_l^b}^l$. We will see that the effect of these closures remains even after considering the local mixture model (section 5) and its homogenised version (section 6).

4.2. From phase velocities to mixture and relative velocities

The relative velocity, mixture velocity and mixture momentum are defined as

$$\overline{\mathbf{u}}_r = \overline{\mathbf{u}}_v^v - \overline{\mathbf{u}}_l^l \tag{11a}$$

$$\overline{\mathbf{u}}_m = c\overline{\mathbf{u}}_v^v + (1-c)\overline{\mathbf{u}}_l^l \tag{11b}$$

$$\rho_m \overline{\mathbf{u}}_m = \alpha\rho_v \overline{\mathbf{u}}_v^v + (1-\alpha)\rho_l \overline{\mathbf{u}}_l^l \tag{11c}$$

where $\rho_m = \alpha\rho_v + (1-\alpha)\rho_l$ is the mixture density and c is the vapour mass fraction. $\overline{\mathbf{u}}_m$ is the centre of mass velocity called *barycentric velocity*. c is related to the void fraction (noted α instead of α_v to lighten the notations) by the relations

$$c\rho_m = \alpha\rho_v \quad \text{or} \quad c = \frac{\alpha\rho_v}{\alpha\rho_v + (1-\alpha)\rho_l} \tag{12a}$$

$$(1-c)\rho_m = (1-\alpha)\rho_l \quad \text{or} \quad 1-c = \frac{(1-\alpha)\rho_l}{\alpha\rho_v + (1-\alpha)\rho_l} \tag{12b}$$

and the mixture density can also be expressed as:

$$\rho_m = \frac{\rho_l\rho_v}{(1-c)\rho_v + c\rho_l} \tag{12c}$$

Also, phase velocities can be derived from the mixture and relative velocities by:

$$\overline{\mathbf{u}}_v^v = \overline{\mathbf{u}}_m + (1-c)\overline{\mathbf{u}}_r \tag{12d}$$

$$\overline{\mathbf{u}}_l^l = \overline{\mathbf{u}}_m - c\overline{\mathbf{u}}_r \tag{12e}$$

Then, the mixture momentum $\rho_m \overline{\mathbf{u}}_m$ obtained from the sum of momentum equations (7a) and (7b) is driven by [see also 2, Eq. (5.42) p. 103 for more information]

$$\frac{\partial \rho_m \overline{\mathbf{u}}_m}{\partial t} + \nabla \cdot (\rho_m \overline{\mathbf{u}}_m \overline{\mathbf{u}}_m) = -\nabla p_m + \rho_m \mathbf{g} \tag{13}$$
$$- \nabla \cdot \Big(\underbrace{c\rho_m \overline{\mathbf{u}'_\mathbf{v}\mathbf{u}'_\mathbf{v}}^v + (1-c)\rho_m \overline{\mathbf{u}'_\mathbf{l}\mathbf{u}'_\mathbf{l}}^l}_{\mathcal{T}^t\text{: Turbulent}} \underbrace{-\mathcal{T}_l^v - \mathcal{T}_v^v}_{-\mathcal{T}^v\text{: Viscous}} \underbrace{-c(1-c)\rho_m \overline{\mathbf{u}}_r \overline{\mathbf{u}}_r}_{\mathcal{T}^{dr}\text{: Diffusion}} \Big) + \mathbf{M_m}$$

where equation (7c) has been used to reduce the sum of interfacial momentum transfers $\mathbf{M_k}$ to a surface tension force and a pressure imbalance. This pressure imbalance naturally disappears from the mixture momentum because the mixture pressure is consistently defined as $p_m = (1-\alpha)\overline{p}_l^l + \alpha \overline{p}_v^v$ with $\overline{p}_l^l = \overline{p_l^{SP}}^l + \overline{p_l^b}^l$. All the terms responsible for the imbalance in equation (7c) are recovered in this budget either in the mixture pressure gradient ∇p_m or in the mixture momentum source term $\mathbf{M_m}$. The respective effects of $\nabla \overline{p_l^b}^l$ and $\mathbf{M_m}$ are unknown in practical applications and it will be the concern of future works to assess their role based on two-fluid simulations to know if there are conditions where they can cancel each other out. Similarly to the diffusion equation (19) (see section 4.3), the diffusion term connected to the relative velocity $\mathcal{T}^{dr}$ arises in the momentum equation due to the use of the mixture velocity to express the convective term.

Furthermore, the combination of equations (7a) and (7b) can also lead to a second equation, this time driving the behaviour of the relative velocity $\overline{\mathbf{u}}_r$

$$\frac{\partial \overline{\mathbf{u}}_r}{\partial t} + \overline{\mathbf{u}}_v^v \cdot \nabla \overline{\mathbf{u}}_v^v - \overline{\mathbf{u}}_l^l \cdot \nabla \overline{\mathbf{u}}_l^l + \left(\frac{\overline{\mathbf{u}}_v^v}{\alpha_v \rho_v} + \frac{\overline{\mathbf{u}}_l^l}{\alpha_l \rho_l} \right) \Gamma_v = \left(\frac{1}{\rho_l} - \frac{1}{\rho_v} \right) \nabla p_m$$
$$+ \frac{1}{(1-c)\rho_m} \nabla \left(\alpha_l \rho_l \overline{\mathbf{u}'_\mathbf{l}\mathbf{u}'_\mathbf{l}}^l - \alpha_l \overline{\tau_l}^l \right) - \frac{1}{c\rho_m} \nabla \left(\alpha_v \rho_v \overline{\mathbf{u}'_\mathbf{v}\mathbf{u}'_\mathbf{v}}^v - \alpha_v \overline{\tau_v}^v \right)$$
$$+ \frac{1}{c(1-c)\rho_m} \mathbf{M_v^{RANS}} - \frac{1}{(1-c)\rho_m} \mathbf{M_m} + \frac{1}{(1-c)\rho_m} \nabla \left(\alpha_v \overline{p}_r + \overline{p_l^b}^l \right) \tag{14}$$

where mass conservation in each phase (18b) has been used to write the left hand side (LHS) of equation (14) in a non-conservative way. $\Gamma_v = -\overline{\dot{m}_v \delta^i}$ is the interfacial mass flux due to evaporation ($\Gamma_v > 0$ in evaporation, see equation (17)). The effect of surface tension is evidenced by the mixture momentum source $\mathbf{M_m}$ but also through the pressure imbalance $\overline{p}_r = \overline{p}_v^v - \overline{p}_l^l$. Lastly, $\overline{p_l^b}^l$ traduces the effect of bubble obstacles to the flow, thus generating a dedicated pressure gradient force.

Phase velocities in the LHS of equation (14) are expressed in terms of relative and mixture velocities ($\overline{\mathbf{u}}_r$ and $\overline{\mathbf{u}}_m$) using equations (12d) and (12e). After simplifications, one gets the relation

$$\overline{\mathbf{u}}_v^v \cdot \nabla \overline{\mathbf{u}}_v^v - \overline{\mathbf{u}}_l^l \cdot \nabla \overline{\mathbf{u}}_l^l = \overline{\mathbf{u}}_m \cdot \nabla \overline{\mathbf{u}}_r + \overline{\mathbf{u}}_r \cdot \Big(\nabla \overline{\mathbf{u}}_m + (1-2c) \nabla \overline{\mathbf{u}}_r \Big) - (\overline{\mathbf{u}}_r \cdot \nabla c)\, \overline{\mathbf{u}}_r \quad (15)$$

that can be injected into the previous PDE for the relative velocity (equation (14)) to get:

$$\begin{aligned} &\frac{\partial \overline{\mathbf{u}}_r}{\partial t} + \overline{\mathbf{u}}_r \cdot \Big(\nabla \overline{\mathbf{u}}_m + (1-2c) \nabla \overline{\mathbf{u}}_r \Big) + \overline{\mathbf{u}}_m \cdot \nabla \overline{\mathbf{u}}_r - (\overline{\mathbf{u}}_r \cdot \nabla c)\, \overline{\mathbf{u}}_r + \frac{\overline{\mathbf{u}}_m + (1-2c)\overline{\mathbf{u}}_r}{c(1-c)\rho_m} \Gamma_v = \\ &\qquad \left(\frac{1}{\rho_l} - \frac{1}{\rho_v} \right) \nabla p_m + \frac{1}{(1-c)\rho_m} \nabla \cdot \left(\mathcal{T}_l^t - \mathcal{T}_l^v \right) - \frac{1}{c\rho_m} \nabla \cdot \left(\mathcal{T}_v^t - \mathcal{T}_v^v \right) \\ &\quad + \frac{1}{c(1-c)\rho_m} \mathbf{M}_\mathbf{v}^{\mathbf{RANS}} - \frac{1}{(1-c)\rho_m} \mathbf{M_m} + \frac{1}{(1-c)\rho_m} \nabla \left(\alpha_v \overline{p}_r + \overline{p_l^b}^l \right) \end{aligned} \quad (16)$$

Independently of the system of equations considered, the role of interfacial transfers is not fully eliminated. They have disappeared from the mixture momentum equation (13) as only the mixture is considered, but their effect has to be accounted for in the closure of the relative velocity $\overline{\mathbf{u}}_r$. These closures are of paramount importance to determine the distribution of void fraction, in particular in the plane orthogonal to the flow; in turn, this distribution will play a key role during the modelling of dispersive terms at the macroscopic scale, in the homogeneous description (section 6).

4.3. Total and vapour mass conservations

The two-phase flow can either be described for each phase separately, or alternatively, one can consider the conservation of total mass and vapour mass separately. The latter option is equivalent but it is in closer agreement with the description of mixture velocity and momentum introduced in section 4.2.

Based on the local equations for mass and interfacial evolution (equations (1a) and (1b)), application of the statistical average leads to mass conservation in each phase:

$$\frac{\partial \alpha_k \rho_k}{\partial t} + \nabla \cdot \left(\alpha_k \rho_k \overline{\mathbf{u}}_k^k\right) = \Gamma_k = -\overline{\dot{m}_v \mathbf{n}_v \cdot \mathbf{n}_k \delta^i} \quad \text{with} \quad k \in [l, v] \tag{17}$$

Summing equation (17) over both phases leads to the total mass conservation while this equation written for the vapour phase governs vapour mass conservation. Expressed in terms of mixture variables (with the help of relations (12a) and (12d)), conservation of total and vapour mass are then given by:

$$\frac{\partial \rho_m}{\partial t} + \nabla \cdot (\rho_m \overline{\mathbf{u}}_m) = 0 \tag{18a}$$

$$\frac{\partial \rho_m c}{\partial t} + \nabla \cdot \left(\rho_m c \overline{\mathbf{u}}_m + \rho_m c(1-c)\overline{\mathbf{u}}_r\right) = \Gamma_v \tag{18b}$$

Equation (18b) is also known as the void propagation equation widely used by Wallis [11]. It expresses the change in vapour mass fraction c and involves a diffusion process with a diffusion velocity $\overline{\mathbf{u}}_{v\to m} = \overline{\mathbf{u}}_v^v - \overline{\mathbf{u}}_m = (1-c)\overline{\mathbf{u}}_r$ defined as the relative velocity of the vapour phase with respect to the centre of mass of the mixture [2, pp. 87-88]. Using the relation $\overline{\mathbf{u}}_{v\to m} = (1-c)\overline{\mathbf{u}}_r$, diffusion due to the velocity difference is exhibited:

$$\frac{\partial \rho_m c}{\partial t} + \nabla \cdot (\rho_m c \overline{\mathbf{u}}_m) = -\nabla \cdot (\rho_m c \overline{\mathbf{u}}_{v\to m}) + \Gamma_v \tag{19}$$

The origin of the apparent diffusion of vapour is related to the convection being based on the mixture centre of mass velocity. Alternately, if the velocity $\overline{\mathbf{u}}_v^v$ of the vapour centre of mass is rebuilt from equation (12d), a simple convection equation is recovered:

$$\frac{\partial \rho_m c}{\partial t} + \nabla \cdot (\rho_m c \overline{\mathbf{u}}_v^v) = \Gamma_v \tag{20}$$

Lastly, using the total mass conservation (18a), vapour mass conservation can also be expressed as:

$$\frac{\partial c}{\partial t} + \overline{\mathbf{u}}_m \nabla c = -\frac{1}{\rho_m} \nabla \cdot \left(\rho_m c(1-c)\overline{\mathbf{u}}_r\right) + \Gamma_v \tag{21}$$

This equation reveals that phase separation is created by the relative velocity. It plays a key role in the cross-flow distribution of void fraction. Depending on the variations of this component of the relative velocity, the divergence in equation (21) can have very different and complex implications, some of which are discussed in the following section.

4.4. Discussions on the relative velocity and phase separation

The relative velocity is a central issue to the modelling of complex two-phase flows. It characterises the intensity of the mechanical coupling between the phases. It affects the void fraction level; it can also be responsible for phase separation or mixing depending on the intensity of the interfacial transfers involved. The governing equation for the relative velocity (equation (16)) is very complex, and it involves several kinds of mechanisms.

In the direction of gravity, relative velocity is classically considered; it results from the drag force in opposition to buoyancy. However, relative velocity also exists in the plane orthogonal to gravity for establishing two-phase flows; it is then due to lift and dispersion forces (among others). In the following, we briefly discuss the impact of the relative velocity and interfacial forces in different directions before reaching the final simplified set of equations describing the local time-averaged two-phase mixture.

4.4.1. Drag and buoyancy

In the direction of the flow and of gravity, two-phase equilibrium is mostly governed by the competition between drag and buoyancy forces. In established flows and at steady-state, streamwise gradients disappear from equation (16) except for the pressure contribution which can be split into dynamic ($\overline{p_l^\star}^l$) and hydrostatic contributions

$$\overline{p}_l^l = \overline{p_l^{SP}}^l + \overline{p_l^b}^l = \overline{p_l^\star}^l + \rho_m \mathbf{g} \cdot \mathbf{x} \tag{22}$$

where $\mathbf{x}$ is the local position vector considered and ρ_m is the local mixture density. For simplicity, let us consider an established pipe flow in cylindrical coordinates (r, z) for the radial and streamwise directions respectively. For an established flow, the liquid pressure gradient $\lambda = \partial \overline{p}_l^l / \partial z$ is independent of the radial position r, so that we have

$$\frac{\partial \overline{p}_l^l}{\partial z} = \lambda = \frac{\partial \overline{p_l^\star}^l}{\partial z}(r) + \rho_m(r) g_z \tag{23}$$

where g_z is the axial component of gravity. Then, the dynamic part $\overline{p_l^\star}^l$ evolves as

$$\overline{p_l^\star}^l(r,z) = \lambda z - g_z z \rho_m(r) = \lambda z - g_z z(\rho_l + \Delta\rho\alpha(r)) \tag{24}$$

if we also assume constant phase densities such that the mixture density ρ_m is simply expressed as $\rho_m = \rho_l + \alpha(r)\Delta\rho$, with $\Delta\rho = \rho_l - \rho_v$. This relation demonstrates the necessary consistency between $\overline{p_l^\star}^l$ and $\alpha(r)$ for established flows. Consequently, a lateral pressure gradient $\partial\overline{p_l^\star}^l/\partial r$ arises from void fraction inhomogeneities. It is perfectly balanced by the void fraction profile so that the radial pressure gradient $\partial\overline{p_l^{SP}}^l/\partial r = 0$. Note that this relation strongly couples the main stream direction with cross-flow directions.

The pressure gradient is the only gradient contribution that remains in the streamwise direction. From the definition of the mixture pressure, it is expressed as:

$$\nabla p_m = \nabla\overline{p_l^{SP}}^l + \nabla\left((1-\alpha)\overline{p_l^b}^l\right) + \alpha\nabla\overline{p}_r + \overline{p}_r\nabla\alpha \tag{25}$$

For established flows, the gradients vanish except for the hydrostatic contribution which is mostly carried by $\overline{p_l^{SP}}^l$. The streamwise contribution then reduces to $\partial\overline{p_l^{SP}}^l/\partial z$ alone. As a consequence, equation (16) simply becomes for the streamwise component of established flows:

$$0 = \left(\frac{1}{\rho_l} - \frac{1}{\rho_v}\right)\frac{\partial\overline{p_l^{SP}}^l}{\partial z} + \left(\frac{1}{\alpha_v\rho_v} + \frac{1}{\alpha_l\rho_l}\right)M_{vz}^{RANS} - \frac{1}{\alpha_l\rho_l}M_{mz} \tag{26}$$

Neglecting surface tension effects ($M_{mz} = 0$) and the liquid pressure induced by the bubbles ($\overline{p_l^b}^l = 0$), and using equation (23), this relation simplifies further to show the classical equilibrium between interfacial forces (then reduced only to the drag force in this direction, $M_{vz}^{RANS} = M_z^D$) and buoyancy:

$$\left(\frac{1}{\alpha_v\rho_v} + \frac{1}{\alpha_l\rho_l}\right)M_{vz}^{RANS} = -\left(\frac{1}{\rho_l} - \frac{1}{\rho_v}\right)\left(\rho_m g_z + \frac{\partial\overline{p_l^\star}^l}{\partial z}\right) \tag{27}$$

Classically, the drag force is related to the square of the relative velocity by

$$\mathbf{M^D} = -\frac{3}{4d_b}\alpha_v C_D \rho_l |\mathbf{u_r}|\mathbf{u_r} \tag{28}$$

where C_D is the drag coefficient and d_b the bubble mean diameter. Under those assumptions, the balance (27) can be exploited to derive the effective drag coefficient in turbulent flows from the knowledge of the relative velocity:

$$\frac{3}{4d_b}C_D\rho_l|\mathbf{u_r}|u_{rz} = \alpha_l\left(\rho_l-\rho_v\right)\left(g_z+\frac{1}{\rho_m}\frac{\partial\overline{p_l^\star}^l}{\partial z}\right) = \alpha_l\left(\rho_l-\rho_v\right)\frac{\lambda}{\rho_m} \tag{29}$$

Alternately, it provides a closure relation for the relative velocity from the knowledge of the drag coefficient. This path is a classical option to derive the relative velocity in the drift flux closure. Usually, the dynamic pressure contribution ($\overline{p_l^\star}^l$) is neglected in front of the hydrostatic gradient due to gravity.

4.4.2. Lateral distribution of void fraction

In order to provide an appropriate description of the system, we assume in this part of the analysis that $\overline{\mathbf{u}}_r$ is closed by a relation of the form

$$\overline{\mathbf{u}}_r = K_D\mathbf{e}_g + K_L\mathbf{e}_\omega + K_{Disp}\mathbf{e}_{\nabla\alpha} \tag{30}$$

where K_D, K_L and K_{Disp} are modelled by closure relations whose expressions depend on the formulation of the drag, lift and dispersion forces respectively, and $\mathbf{e}_g$, $\mathbf{e}_\omega$, $\mathbf{e}_{\nabla\alpha}$ are respectively directions provided by the gravity, the curl of the liquid velocity $\omega_l = \nabla\wedge\overline{\mathbf{u}}_l^l$ and the void-fraction gradient. The curl of the liquid velocity $\overline{\mathbf{u}}_l^l$ still needs to be related to the variables of the system considered (in particular when using the mixture velocity as a main variable), but for moderate void fractions and relative velocities, it could be assimilated to the curl $\nabla\wedge\overline{\mathbf{u}}_m$ by a rather strong simplification of relation (12e).

Using a closure for the relative velocity $\overline{\mathbf{u}}_r$ as equation (30), the vapour mass conservation equation (21) becomes:

$$\frac{\partial c}{\partial t}+\overline{\mathbf{u}}_m\nabla c = -\frac{1}{\rho_m}\nabla\cdot\left[\rho_m c(1-c)\left(K_D\mathbf{e}_g+K_L\mathbf{e}_\omega+K_{Disp}\mathbf{e}_{\nabla\alpha}\right)\right] \tag{31}$$

The drag contribution $K_D\mathbf{e}_g$ is responsible for stratification in horizontal or inclined flows. The lift contribution will be particularly important in high-shear regions. Depending on the sign of the lift force, which in turns depends on the bubbles' deformability and Weber number, it can act in opposite directions, either creating dispersion of void fraction or contributing to the accumulation of bubbles. Lastly, the term $K_{Disp}\mathbf{e}_{\nabla\alpha}$ arises from both

laminar and turbulent dispersion forces; it contributes to the homogenisation of the void fraction. With all these complicated mechanisms at play, equation (31) governs the vapour distribution in the flow. These competing effects are in particular determinant in the detection of a transition from wall- to core-peaked flows, which is a key ingredient to the proper modelling of CHF prediction. The accurate modelling of equation (31) is a central element that determines the capabilities of a mixture model, in particular when concerns arise with respect to fine predictions of the void fraction spreading into the cross-flow plane. It is really challenging, yet essential to these kinds of approaches, to be able to provide a closure to equation (30) valid in most configurations; indeed, this limit is a key-point that determines the applicability range of the global model.

4.5. Summary of the (complete) two-fluid model

In order to complete the local statistical description of the system, it is necessary to provide conservation equations for the energy in each phase. These equations are easily derived by application of the statistical average to the local instantaneous phase-equations contained in the equation system (1). As it is not the main concern of the present article and it can be easily found in the literature [2, 3], we directly give the complete system encompassing the momentum equations (7a) and (7b).

Two alternatives are possible either considering conservation in each phase, or regarding total and vapour balances. The systems obtained are summarised as follows. If each phase is considered, statistically-averaged equations for mass, momentum and energy writes for $k \in [l, v]$

$$\frac{\partial \alpha_k \rho_k}{\partial t} + \nabla \cdot \left(\alpha_k \rho_k \overline{\mathbf{u}}_k^k \right) = \Gamma_k, \tag{32a}$$

$$\frac{\partial \alpha_k \rho_k \overline{\mathbf{u}}_k^k}{\partial t} + \nabla \cdot \left(\alpha_k \rho_k \overline{\mathbf{u}}_k^k \overline{\mathbf{u}}_k^k \right) = -\alpha_k \nabla \overline{p_l^{SP}}^l + \nabla \cdot \left(\mathcal{T}_k^v - \mathcal{T}_k^t \right) + \alpha_k \rho_k \mathbf{g} + \mathbf{M}_\mathbf{k}^{\mathbf{RANS}}, \tag{32b}$$

$$\frac{\partial \alpha_k \rho_k \overline{h}_k^k}{\partial t} + \nabla \cdot \left(\alpha_k \rho_k \overline{\mathbf{u}}_k^k \overline{h}_k^k \right) = \frac{\partial \alpha_k \overline{p_k}^k}{\partial t} + \nabla \cdot \left(\alpha_k \lambda_k \nabla \overline{T}_k^k + \mathbf{Q}_k^c - \mathbf{Q}_k^t \right) + \mathbf{Q}_k^i, \tag{32c}$$

where $\mathbf{Q}_k^t = \alpha_k \rho_k \overline{\mathbf{u}_k' h_k'}^k$ is the turbulent heat flux and $\mathbf{Q}_k^i$ is the interfacial energy transfer (satisfying the interfacial jump condition $\mathbf{Q}_l^i + \mathbf{Q}_v^i = 0$) defined by $\mathbf{Q}_k^i = \overline{[\dot{m}_k h_k \mathbf{n}_k - \lambda_k \nabla T_k] \cdot \nabla \chi_k}$. The correlation heat flux $\mathbf{Q}_k^c$ arises from

the cross-correlation between the interfacial temperature and the interface orientation $\mathbf{n}_k$:

$$\mathbf{Q}_k^c = \lambda_k \left(\overline{T}_k^k \nabla \alpha_k - \overline{T_k \nabla \chi_k} \right) \tag{33}$$

Similarly to the viscous diffusion in equation (6), this term is not spelled out in classical derivations of two-fluid models; it is therefore neglected without further justification. We can observe from this expression that even when the interfacial temperature is assumed constant and equal to the saturation temperature, the cross-correlation remains different from zero, but it is then fully expressed in terms of main variables: $\mathbf{Q}_k^c = \lambda_k \left(\overline{T}_k^k - T^i \right) \nabla \alpha_k$. A magnitude assessment on practical cases would be interesting to determine the influence of this contribution.

Provided that the equation system (32) is supplemented with closure relations for Γ_v, $\mathcal{T}_k^t$, $\mathcal{T}_k^v$, $\mathbf{M}_\mathbf{k}^{\mathbf{RANS}}$, and for the fluxes $\mathbf{Q}_k^c$, $\mathbf{Q}_k^t$, $\mathbf{Q}_k^i$, and also with the necessary relations between the different pressures considered, it can be solved to describe the evolution of the two-phase system $(\alpha_v, \overline{\mathbf{u}}_l^l, \overline{\mathbf{u}}_v^v, \overline{p_l^{SP}}^l, \overline{h}_l^l, \overline{h}_v^v)$.

The alternative system considering the mixture density ρ_m, the vapour mass concentration c, the mixture velocity $\overline{\mathbf{u}}_m$ and the relative velocity $\overline{\mathbf{u}}_r$ is obtained from equations (18a), (19), (13) and (16):

$$\frac{\partial \rho_m}{\partial t} + \nabla \cdot (\rho_m \overline{\mathbf{u}}_m) = 0, \tag{34a}$$

$$\frac{\partial \rho_m c}{\partial t} + \nabla \cdot (\rho_m c \overline{\mathbf{u}}_m) = -\nabla \cdot (\rho_m c \overline{\mathbf{u}}_{v \to m}) + \Gamma_v, \tag{34b}$$

$$\frac{\partial \rho_m \overline{\mathbf{u}}_m}{\partial t} + \nabla \cdot (\rho_m \overline{\mathbf{u}}_m \overline{\mathbf{u}}_m) = -\nabla p_m + \rho_m \mathbf{g} - \nabla \cdot \left(\mathcal{T}^t - \mathcal{T}^v + \mathcal{T}^{dr} \right) + \mathbf{M_m} \tag{34c}$$

$$\begin{aligned} \frac{\partial \overline{\mathbf{u}}_r}{\partial t} + \overline{\mathbf{u}}_r \cdot \left(\nabla \overline{\mathbf{u}}_m + (1-2c) \nabla \overline{\mathbf{u}}_r \right) + \overline{\mathbf{u}}_m \cdot \nabla \overline{\mathbf{u}}_r - (\overline{\mathbf{u}}_r \cdot \nabla c) \, \overline{\mathbf{u}}_r + \frac{\overline{\mathbf{u}}_m + (1-2c) \overline{\mathbf{u}}_r}{c(1-c)\rho_m} \Gamma_v = \\ \left(\frac{1}{\rho_l} - \frac{1}{\rho_v} \right) \nabla p_m + \frac{1}{(1-c)\rho_m} \nabla \cdot \left(\mathcal{T}_l^t - \mathcal{T}_l^v \right) - \frac{1}{c \rho_m} \nabla \cdot \left(\mathcal{T}_v^t - \mathcal{T}_v^v \right) \\ + \frac{1}{c(1-c)\rho_m} \mathbf{M}_\mathbf{v}^{\mathbf{RANS}} - \frac{1}{(1-c)\rho_m} \mathbf{M_m} + \frac{1}{(1-c)\rho_m} \nabla \left(\alpha_v \overline{p}_r + \overline{p_l^b}^l \right). \end{aligned} \tag{34d}$$

For the energy, this system can be completed by any suitable combination of two equations that can be phase enthalpy conservations, or the governing equation for the mixture enthalpy, or one for the enthalpy difference, or

a simplifying assumption such as the equality of a phase enthalpy to the saturation value. These aspects are not discussed in more detail here as they are not the main focus of the present contribution.

In the following, we first proceed to a model reduction with the elimination of the transport equation for the relative velocity; then, a macroscopic model is derived by volume averaging.

5. Model reduction for the local time-averaged description

This section explains the simplifications applied to the two-fluid model in order to obtain the mixture model. This reduction of the model comes with the need for an additional closure relation for the relative velocity.

5.1. Several choices for systems of time-averaged equations at the local scale

In this section, we focus on the system dynamics, thermal simplifications being out of the scope of this article. Using a set of equations to govern the mixture momentum and the relative velocity as in the equation system (34) is formally equivalent to the usage of equations governing phase-variables as in the equation system (32). When mixture momentum and relative velocity equations are completed by an equation for the total mass conservation (as equation (34a)) and one for the vapour mass conservation (equation (34b)) for instance, the resulting system of equations can be solved provided that closure relations for the Reynolds stresses ($\overline{\mathbf{u}_\mathbf{l}'\mathbf{u}_\mathbf{l}'}^{l}$ and $\overline{\mathbf{u}_\mathbf{v}'\mathbf{u}_\mathbf{v}'}^{v}$), the viscous contributions ($\mathcal{T}_l^v$ and $\mathcal{T}_v^v$), the interfacial transfers ($\mathbf{M}_\mathbf{v}^{\mathbf{RANS}}$) and the surface tension effects ($\mathbf{M}_\mathbf{m}$, $\overline{p}_r$ and $\overline{p_l^b}^{l}$) are given. In this article, surface tension effects are defined in the broad sense as they also include pressure variations induced by surface tension or by the presence of inclusions. This approach leads to a set of 6 PDEs (accounting for an energy equation for each phase) that are classically used to solve the two-fluid model. It is theoretically equivalent to the resolution of two equations of mass and two for the momentum of each phase (plus two additional equations for the phase energies in the complete case). The two approaches simply lead to different numerical strategies that can be more or less efficient depending on the intrinsic coupling between the equations into the system.

Instead of this complete and demanding approach, one can decide to reduce the size of the system by considering only the PDE for the mixture momentum (13). It is then necessary to provide an appropriate closure for

the relative velocity in replacement of equation (16). One of the main advantages of this choice is that it eliminates the need for closure relations for the interfacial transfers $\mathbf{M_v^{RANS}}$ but the direct consequence is that this closure should be capable of including complex phenomena in the lateral direction that result in particular from these interfacial transfers. Usually, one important weakness of this approach is that it considers only the relative velocity created by the competing drag and buoyancy forces and it totally neglects other forces (such as lift, dispersion and wall effects) responsible for the lateral redistribution of void fraction. Then, the physical effects of lateral forces have to be empirically introduced into the system of equations to recover more physical results. In this article, we clarify their meaning by establishing the theoretical expression of these empirical models based on the local description of the flow. We will see how they are related to interfacial forces and to the relative velocity.

5.2. The local drift-flux model: a simplified 4 equations model

Depending on the strength of the coupling between the two phases, one may reduce the number of PDE considered. The counterpart of this simplification of the system is the modelling of additional closure relations. Here, we consider a flow of dispersed bubbles where the two phases are strongly coupled dynamically. Then, instead of solving for a momentum budget for each phase, we will only consider the mixture, and we will introduce a closure relation for the relative velocity between the phases defined as $\overline{\mathbf{u}}_r = \overline{\mathbf{u}}_v^v - \overline{\mathbf{u}}_l^l$. This leads to a description of the mixture known as diffusion model or mixture model [2, p. 103]. It is based on differential equations of the local statistically-averaged two-fluid system

$$\frac{\partial \rho_m}{\partial t} + \nabla \cdot (\rho_m \overline{\mathbf{u}}_m) = 0, \tag{35a}$$

$$\frac{\partial \rho_m c}{\partial t} + \nabla \cdot (\rho_m c \overline{\mathbf{u}}_m) = -\nabla \cdot (\rho_m c \overline{\mathbf{u}}_{v\to m}) + \Gamma_v, \tag{35b}$$

$$\frac{\partial \rho_m \overline{\mathbf{u}}_m}{\partial t} + \nabla \cdot (\rho_m \overline{\mathbf{u}}_m \overline{\mathbf{u}}_m) = -\nabla p_m + \rho_m \mathbf{g} - \nabla \cdot \left(\mathcal{T}^t - \mathcal{T}^v + \mathcal{T}^{dr}\right) + \mathbf{M_m}, \tag{35c}$$

completed by a necessary relation to close the relative velocity $\overline{\mathbf{u}}_r$ in replacement of the exact governing equation (34d). This closure leads to the diffusion velocity $\overline{\mathbf{u}}_{v\to m}$ and as a result, it provides a closure to consistently

express the diffusion stress due to relative velocity $\mathcal{T}^{dr}$, as defined in equation (13). It is also necessary to supplement the system with expressions for the interfacial mass transfer Γ_v, the turbulent Reynolds stresses $\mathcal{T}^t$, the viscous stresses $\mathcal{T}^v$ (that are not naturally defined in terms of the mean velocity) and the surface tension effect $\mathbf{M_m}$.

From the energy point-of-view, the vapour phase can be assumed at thermal equilibrium with the saturation temperature of the system in flows of small dispersed bubbles. Otherwise, an equation for the mixture enthalpy can be obtained from the sum of equation (32c) on each phase. In flows with heat transfer and phase-change, mechanical effects are mostly insignificant [2, pp. 107-108]. Due to the difference in phase velocities, diffusion transport of thermal energy becomes an important effect to consider as it is proportional to the relative velocity and to the difference between the phase enthalpies (close to the latent heat). It is interesting to note that even if each phase energy is considered separately instead of considering the mixture enthalpy, the diffusion transport is still an important mechanism; indeed, it arises from the necessary use of the mixture velocity in the convective term of the mixture model. Therefore, following the same methodology as before, the balance for phase enthalpies given by equation (32c) leads to the governing equation for the mixture enthalpy h_m:

$$\frac{\partial \rho_m h_m}{\partial t} + \nabla \cdot (\rho_m \overline{\mathbf{u}}_m h_m) = \frac{\partial p_m}{\partial t} + \nabla \cdot \left(\mathbf{Q}^f + \mathbf{Q}^c - \mathbf{Q}^t - \mathbf{Q}^d \right), \qquad (35d)$$

Here, we used the interfacial equilibrium $\mathbf{Q}_l^i + \mathbf{Q}_v^i = 0$. Mixture enthalpy is defined without a velocity-weighting $h_m = \alpha_l \rho_l \overline{h}_l^l + \alpha_v \rho_v \overline{h}_v^v$. Diffusion of each phase with respect to the mixture centre of mass then causes the appearance of a diffusive flux defined as

$$\mathbf{Q}^d = \sum_{k=l,v} \alpha_k \rho_k \overline{h}_k^k \overline{\mathbf{u}}_{k\to m} = \rho_m c(1-c) \overline{\mathbf{u}}_r \left(\overline{h}_v^v - \overline{h}_l^l \right) \qquad (36)$$

where $\overline{\mathbf{u}}_{k\to m} = \overline{\mathbf{u}}_k^k - \overline{\mathbf{u}}_m$ is the difference of the phase velocity to the mixture velocity. Modelling this diffusion transport $\mathbf{Q}^d$ is essential because of the large difference of phase enthalpies; assuming this enthalpy difference close to the latent heat, the closure of the relative velocity provides a definition for this flux. In addition, closure relations are required for the mixture turbulent heat flux $\mathbf{Q}^t = \mathbf{Q}_l^t + \mathbf{Q}_v^t$, for the mixture correlation heat flux

$\mathbf{Q}^c = \mathbf{Q}^c_l + \mathbf{Q}^c_v$ and for the conduction heat flux $\mathbf{Q}^f$ representing an equivalent of the Fourier's conduction law for the mixture:

$$\mathbf{Q}^f = \sum_{k=l,v} \alpha_k \lambda_k \nabla \overline{T}^k_k \tag{37}$$

The convective terms $\mathbf{Q}^f$ and $\mathbf{Q}^c$ can be rearranged together. They require models to approach the phase temperatures $\overline{T}^k_k$ and the microscopic correlation $\overline{T_i \nabla \chi_v}$:

$$\mathbf{Q}^f + \mathbf{Q}^c = \sum_{k=l,v} \lambda_k \nabla \left(\alpha_k \overline{T}^k_k \right) + [\![\lambda]\!] \, \overline{T_i \nabla \chi_v} \tag{38}$$

If the interfacial temperature is considered uniform (for instance taken as a constant saturation temperature at interfaces at thermo-dynamical equilibrium), the microscopic correlation is then naturally expressed in terms of the variables of the system and it is proportional to the gradient of void fraction. For the other part, phase temperatures require the knowledge of phase enthalpies combined with relations between $\overline{h}^k_k$ and $\overline{T}^k_k$. Lastly, if the phases are considered compressible, the equation of state of the mixture providing a link of the form $\rho_m = f(p_m, h_m)$ can be difficult to establish; in particular, if a pressure imbalance is considered and the equations of state for each phase are of the form $\rho_k = f(\overline{p}^k_k, \overline{h}^k_k)$. The modelling choice selected for the pressure imbalance will also affect the solution in that indirect way.

6. Homogenisation: volume averaging

Homogenisation is used to describe the two-phase flow at a larger scale. It relies on space-averaging the local system of equations to describe it at the macroscopic scale [49]. We consider the space filter $\langle\ \rangle$ of any variable ξ given by

$$\langle \xi \rangle (\mathbf{x}, t) = \frac{1}{V} \int_V \xi(\mathbf{x}', t) dV, \tag{39}$$

where the averaging volume V is independent of the position. We also introduce the indicator function of the fluid phase χ_f equal to unity in the fluid domain and zero otherwise. Besides, walls are associated to a Dirac delta-distribution δ_w and their unit normal $\mathbf{n}_w$ (oriented outward from the fluid into the wall) is defined by $\nabla \chi_f = -\delta_w \mathbf{n}_w$. The porosity $\phi = \langle \chi_f \rangle = V_f / V$ gives the ratio of the fluid volume V_f to the averaging volume V. Similarly

to Whitaker [6], the intrinsic filtering is defined from the following weighted-average:

$$\langle \xi \rangle_f (\mathbf{x}, t) = \frac{\langle \xi \chi_f \rangle}{\langle \chi_f \rangle} = \frac{1}{V_f} \int_{V_f} \xi(\mathbf{x}', t) dV. \tag{40}$$

Finally, any quantity ξ is decomposed into its filtered quantity $\langle \xi \rangle_f$ and a spatial deviation $\delta_s \xi$: $\xi = \langle \xi \rangle_f + \delta_s \xi$. Contrary to the statistical average, the filter does not commute with space derivatives and it is not idempotent [6]. For motionless walls, the following rules apply [50]:

$$\phi \langle \nabla \xi \rangle_f = \phi \nabla \langle \xi \rangle_f + \phi \langle \delta_s \xi \ \delta_w \mathbf{n} \rangle_f , \tag{41a}$$

$$\langle \chi_f \nabla \xi \rangle = \phi \langle \nabla \xi \rangle_f = \nabla (\phi \langle \xi \rangle_f) + \phi \langle \xi \ \delta_w \mathbf{n} \rangle_f , \tag{41b}$$

$$\phi \left\langle \frac{\partial \xi}{\partial t} \right\rangle_f = \phi \frac{\partial \langle \xi \rangle_f}{\partial t} = \frac{\partial \phi \langle \xi \rangle_f}{\partial t}. \tag{41c}$$

6.1. Particular filters

6.1.1. Dimensionality reduction: plane channel application

As a particular example of space-averaging operator $\langle\rangle$, one can consider a flow in a narrow rectangular channel, with parallel walls at $y = -e/2$ and $y = e/2$. The fluid indicator function is then $\chi_f = 1$ in the fluid domain, *i. e.*, $-e/2 \leq y \leq e/2$, and $\chi_f = 0$ in the solid structures. In that case, one can consider the application of the space-averaging operator defined as the average over the small channel gap e:

$$\langle \xi \rangle (x, z, t) = \frac{1}{e} \int_{-e/2}^{e/2} \xi(\mathbf{x}', t) dy \tag{42}$$

After the application of this space-averaging operator, the problem description reduces to two dimensions. Profiles along the channel width are unresolved and sub-grid correlations appear due to non-linearities, products of variables or gradient operators. Due to the dimensionality reduction of this particular filter, the filter is naturally idempotent as one can easily show that

$$\langle \langle \xi \rangle \rangle = \langle \xi \rangle$$

as a result of the independence of $\langle \xi \rangle$ to y, which also means that the deviation $\delta_s \xi(x, y, z)$ is centred with respect to that averaging:

$$\langle \delta_s \xi \rangle = 0$$

In addition, this filtering on y-direction naturally commutes with $x-$ and z-derivatives.

6.1.2. Scale separation

For a more general filter, it is idempotent and the deviation is centred with respect to it if there is a scale separation such that

$$l_\xi \lesssim r_0 \lesssim L_{\langle\xi\rangle}$$

where the characteristic sizes r_0, l_ξ and $L_{\langle\xi\rangle}$ corresponds respectively to the filter kernel, the microscopic scale of variation of the variable ξ and the macroscopic scale of variation of its filtered counterpart $\langle\xi\rangle$. In the case of the particular one-dimensional filter defined above, the splitting between directions replaces scale separation.

6.2. Favre averaging: density- and fluid-weighted average

As the mixture density strongly varies as a result of variations in vapour concentration, it is more convenient to define a Favre averaging operator weighted by both the mixture density ρ_m and the fluid phase indicator function χ_f, along with the definition of the corresponding deviation:

$$\widetilde{\xi} = \frac{\langle\chi_f\rho_m\xi\rangle}{\langle\chi_f\rho_m\rangle} = \frac{\phi\,\langle\rho_m\xi\rangle_f}{\phi\,\langle\rho_m\rangle_f} = \frac{\langle\rho_m\xi\rangle_f}{\rho_M} \tag{43a}$$

$$\delta\xi = \xi - \widetilde{\xi} \tag{43b}$$

$\rho_M = \langle\rho_m\rangle_f$ is the macroscopic mixture density (identified by the capital subscript $_M$). From these definitions, we can demonstrate that for two fields ξ and ζ, we have under the assumption of scale separation or for an idempotent filter:

$$\langle\chi_f\rho_m\xi\zeta\rangle = \phi\rho_M\widetilde{\xi}\,\widetilde{\zeta} + \phi\,\langle\rho_m\delta\xi\,\delta\zeta\rangle_f = \phi\rho_M\left(\widetilde{\xi}\,\widetilde{\zeta} + \widetilde{\delta\xi\,\delta\zeta}\right) \tag{44}$$

6.3. Macroscopic mixture model

Motionless walls are considered. Multiplying the mixture model given in the equation system (35) by the fluid indicator function χ_f and applying this

filter leads to

$$\phi\frac{\partial\left\langle\rho_m\right\rangle_f}{\partial t}+\nabla\cdot\left(\phi\left\langle\rho_m\overline{\mathbf{u}}_m\right\rangle_f\right)=0, \tag{45a}$$

$$\phi\frac{\partial\left\langle\rho_m c\right\rangle_f}{\partial t}+\nabla\cdot\left(\phi\left\langle\rho_m c\overline{\mathbf{u}}_m\right\rangle_f\right)=-\nabla\cdot\left(\phi\left\langle\rho_m c\overline{\mathbf{u}}_{v\to m}\right\rangle_f\right)+\phi\left\langle\Gamma_v\right\rangle_f, \tag{45b}$$

$$\begin{aligned}\phi\frac{\partial\left\langle\rho_m\overline{\mathbf{u}}_m\right\rangle_f}{\partial t}+\nabla\cdot\left(\phi\left\langle\rho_m\overline{\mathbf{u}}_m\overline{\mathbf{u}}_m\right\rangle_f\right)&=-\phi\left\langle\nabla p_m\right\rangle_f+\phi\left\langle\rho_m\right\rangle_f\mathbf{g}\\ -\nabla\cdot\left(\phi\left\langle\mathcal{T}^t\right\rangle_f+\phi\left\langle\mathcal{T}^v\right\rangle_f+\phi\left\langle\mathcal{T}^{dr}\right\rangle_f\right)-\phi\left\langle\mathcal{T}^v\ \delta_w\mathbf{n}\right\rangle_f&+\phi\left\langle\mathbf{M_m}\right\rangle_f.\end{aligned} \tag{45c}$$

The combination of equation (41b) and of the condition of no-slip velocity at the walls was used to obtain equation (45a). We assume that the no-slip condition at the wall applies to both $\overline{\mathbf{u}}_m$ and $\overline{\mathbf{u}}_r$ (and transitively to $\overline{\mathbf{u}}_{v\to m}$). Besides, the turbulent stress goes to zero at the walls leading to the deletion of the wall/turbulent contribution $\mathcal{T}^t\ \delta_w$. The contribution of the diffusion term $\left\langle\mathcal{T}^{dr}\right\rangle_f$ at the wall also vanishes because the velocity of each phase goes to zero at the wall when no-slip is considered; then, we have $\overline{\mathbf{u}}_r\,\delta_w=0$, thus leading to wall friction effects represented solely by the term $\phi\left\langle\mathcal{T}^v\ \delta_w\mathbf{n}\right\rangle_f$ (and a pressure contribution spilled out below, in equation (48)).

Then, one needs to define the main variables of the system. Similarly to the local mixture (or diffusion) model summarised in section 5.2, we define filtered quantities weighted by the centre of mass. Therefore, we will describe the evolution of the filtered mixture density ρ_M, vapour concentration c_M, centre of mass velocity $\overline{\mathbf{u}}_M$ and filtered pressure p_M defined as:

$$\rho_M=\left\langle\rho_m\right\rangle_f \tag{46a}$$

$$\rho_M\,c_M=\left\langle\rho_m c\right\rangle_f \tag{46b}$$

$$\rho_M\overline{\mathbf{u}}_M=\left\langle\rho_m\overline{\mathbf{u}}_m\right\rangle_f \tag{46c}$$

$$p_M=\left\langle p_m\right\rangle_f \tag{46d}$$

Using equation (44) and the definitions above, the correlation between mean velocity deviations $\delta\overline{\mathbf{u}}_m$ arises from the convective term

$$\left\langle\rho_m\overline{\mathbf{u}}_m\overline{\mathbf{u}}_m\right\rangle_f=\rho_M\overline{\mathbf{u}}_M\overline{\mathbf{u}}_M-\mathbf{D}_M \tag{47}$$

where $\mathbf{D}_M=-\rho_M\widetilde{\delta\overline{\mathbf{u}}_m\delta\overline{\mathbf{u}}_m}$ is the macroscopic dispersion due to local mean velocity profiles. Besides, the pressure term gives rise to a wall contribution:

$$\phi\left\langle\nabla p_m\right\rangle_f=\phi\nabla\left\langle p_m\right\rangle_f+\phi\left\langle\delta_s p_m\ \delta_w\mathbf{n}\right\rangle_f\quad\text{where}\quad\delta_s p_m=p_m-\left\langle p_m\right\rangle_f \tag{48}$$

Therefore, the system describing the selected variables can be obtained from the previous equation system (45)

$$\frac{\partial \rho_M}{\partial t} + \nabla_\phi \cdot (\rho_M \overline{\mathbf{u}}_M) = 0, \tag{49a}$$

$$\frac{\partial \rho_M c_M}{\partial t} + \nabla_\phi \cdot (\rho_M c_M \overline{\mathbf{u}}_M + \rho_M \overline{\mathbf{u}}_D) = \Gamma_M, \tag{49b}$$

$$\frac{\partial \rho_M \overline{\mathbf{u}}_M}{\partial t} + \nabla_\phi \cdot (\rho_M \overline{\mathbf{u}}_M \overline{\mathbf{u}}_M) = -\nabla p_M + \rho_M \mathbf{g} \tag{49c}$$

$$-\nabla_\phi \cdot \left(\mathbf{D}_M + \langle \mathcal{T}^v \rangle_f + \left\langle \mathcal{T}^t \right\rangle_f + \left\langle \mathcal{T}^{dr} \right\rangle_f \right) + \mathbf{M}_\mathbf{M} - \langle \delta_s p_m \ \delta_w \mathbf{n} \rangle_f - \langle \mathcal{T}^v \ \delta_w \mathbf{n} \rangle_f .$$

where $\Gamma_M = \langle \Gamma_v \rangle_f$ is the mean vaporisation term and $\mathbf{M}_\mathbf{M} = \langle \mathbf{M}_\mathbf{m} \rangle_f$ the mean mixture momentum source. The notation $\nabla_\phi \cdot \zeta = \frac{1}{\phi} \nabla \cdot (\phi \zeta)$ is used to represent the divergence operator in case of variable porosity.

In this system, one can see one of the main advantages of the Favre-averaged variables that we have selected. The centre-of-mass definitions cause the exact mass conservation equation of the macroscopic system (equation (49a)) to be totally described in terms of main variables (thanks to the definitions (46a) and (46c)), hence ensuring an accurate mass preservation independently of the quality of the closures selected. This is an important property of the derivation and of the selected choice of macroscopic variables. Unfortunately, the conservation equation for the mass of vapour (49b) cannot be described without closure. It is necessary to introduce a model for a drift velocity which is exactly defined in terms of local variables by:

$$\overline{\mathbf{u}}_D = \underbrace{\widetilde{\delta c \, \delta \overline{\mathbf{u}}_m}}_{\overline{\mathbf{u}}_{D1}} + \underbrace{\widetilde{c(1-c)} \overline{\mathbf{u}}_r}_{\overline{\mathbf{u}}_{D2}} = \widetilde{\delta c \, \delta \overline{\mathbf{u}}_m} + \widetilde{c \overline{\mathbf{u}}_{v \to m}} \tag{50}$$

Therefore, this velocity arises from the correlation between deviations of vapour concentration and mean velocity on one hand, and from the correlation of vapour concentration to the relative velocity on the other.

In the momentum equation, macroscopic dispersion $\mathbf{D}_M$ arises from the cross correlation $\delta \widetilde{\overline{\mathbf{u}}_m \delta \overline{\mathbf{u}}_m}$, that is caused by the local deviations of the mean velocity $\overline{\mathbf{u}}_m$ from its mean value $\overline{\mathbf{u}}_M$. $\mathbf{V} = \langle \mathcal{T}^v \rangle_f$, $\mathbf{T} = \langle \mathcal{T}^t \rangle_f$ and $\mathbf{D}^r = \left\langle \mathcal{T}^{dr} \right\rangle_f$ correspond respectively to the macroscopic viscous, turbulent and diffusion tensors. The diffusion due to the relative velocity $\mathbf{D}^r$ is completed by the similar process of dispersion $\mathbf{D}_M$ due this time to the averaging

process at the basis of the macroscopic description. They all require modelling to close the system, as they involve products of microscopic (local) mean or instantaneous variables. The viscous term $\mathbf{V}$ can be developed using the definition (6) of the (local) mean viscous stresses $\mathcal{T}^v$ in relation to the tensor $\breve{\tau}_k$

$$\mathbf{V} = -\mu_v \nabla_\phi^\dagger \left(\langle \alpha_v \overline{\mathbf{u_v}}^v \rangle_f \right) - \mu_l \nabla_\phi^\dagger \left(\left\langle \alpha_l \overline{\mathbf{u_l}}^l \right\rangle_f \right) \tag{51}$$

using the adherence of both phase velocities at the walls and assuming that each phase viscosity vary weakly with respect to the filter size (*i. e.,* we neglect sub-filter variations of physical properties). An issue similar to the closure of the macroscopic equation for the vapour mass (49b) is encountered, namely the fact that macroscopic velocities are related to the mixture centre of mass. In order to close the viscous term $\mathbf{V}$, it is necessary to express $\langle \alpha_v \overline{\mathbf{u_v}}^v \rangle_f$ and $\left\langle \alpha_l \overline{\mathbf{u_l}}^l \right\rangle_f$ as a function of mixture variables. Cross-correlations identical to those in equation (50) appear. Thus, using the same definition, and assuming weak variations of densities with respect to the filter size, we have:

$$\langle \alpha_v \overline{\mathbf{u_v}}^v \rangle_f = \frac{1}{\rho_v} \left(\langle \rho_m c \overline{\mathbf{u}}_m \rangle_f + \langle \rho_m c \overline{\mathbf{u}}_{v \to m} \rangle_f \right) = \frac{\rho_M}{\rho_v} \left(c_M \overline{\mathbf{u}}_M + \overline{\mathbf{u}}_D \right) \tag{52a}$$

$$\left\langle \alpha_l \overline{\mathbf{u_l}}^l \right\rangle_f = \frac{1}{\rho_l} \left(\langle \rho_m (1-c) \overline{\mathbf{u}}_m \rangle_f + \langle \rho_m c \overline{\mathbf{u}}_{v \to m} \rangle_f \right) = \frac{\rho_M}{\rho_l} \left((1-c_M) \overline{\mathbf{u}}_M - \overline{\mathbf{u}}_{D1} + \overline{\mathbf{u}}_{D2} \right) \tag{52b}$$

As a consequence, the viscous term $\mathbf{V}$ can be closed solely resorting to the closures of $\overline{\mathbf{u}}_{D1}$ and $\overline{\mathbf{u}}_{D2}$ under the current assumptions.

Moreover, the turbulent term traduces the macroscopic effect of the Reynolds stresses. Averaging local CFD simulations could be a useful tool to provide information on its behaviour. The simplest way to model it could be an algebraic relation to the mean shear stress

$$\mathbf{T} = \left\langle c \rho_m \overline{\mathbf{u'_v} \mathbf{u'_v}}^v + (1-c) \rho_m \overline{\mathbf{u'_l} \mathbf{u'_l}}^l \right\rangle_f \approx K_M \mathbf{S_M} \tag{53}$$

where K_M is a tensor set of coefficients and $\mathbf{S_M}$ is the deviatoric part of the macroscopic stress tensor:

$$\mathbf{S_M} = \frac{1}{2} \nabla^\dagger \overline{\mathbf{u}}_M \tag{54}$$

Lastly, the diffusion tensors $\mathbf{D}^r$ corresponds to dispersion effects due to relative velocity

$$\mathbf{D}^r = \langle -c(1-c)\rho_m \overline{\mathbf{u}}_r \overline{\mathbf{u}}_r \rangle_f = -\langle \rho_m c \overline{\mathbf{u}}_{v\to m} \overline{\mathbf{u}}_r \rangle_f \tag{55}$$

Again, fine scale simulations would be beneficial to improve the understanding of this term. It traduces the complex correlation between vapour mass concentration, the relative velocity of the vapour phase to the centre of mass of the mixture $\overline{\mathbf{u}}_{v\to m}$ and the relative velocity $\overline{\mathbf{u}}_r$. This tensor is diagonal.

Besides, pressure loss from wall friction results from the combination of a pressure deviation $\delta_s p_m$ and a viscous contribution. It stresses the importance of sub-filter variations.

In conjunction to the effects of velocity variations and fluctuations and in addition to the influence of relative velocities, one last important element has to be discussed. The macroscopic mixture pressure p_M defined by equation (46d) is selected as a main variable of the system. If a single pressure is considered at the local scale ($\overline{p}_l^l = \overline{p}_v^v = p_m$), then equations of state (EOS) of each phase can be used to assess phase densities provided that the effect of sub-filter variations of pressure on physical properties is assumed negligible or at least linear. In the case of plane channel filtering, it means neglecting non-linear impact of wall-normal pressure variations on densities. Now, if a more complete description of the local scale is considered with a local pressure imbalance, relating the EOS of each phase to the EOS of the mixture becomes more complex because non-linear relations need to be inverted. It is difficult to determine theoretically the influence of the closures selected for the pressure imbalance on the global system resolution including EOS. As a consequence, we plan on using local CFD simulations based on RANS two-fluid models to determine the predominant closures and to hint towards appropriate modelling possibilities. However, it is important to insist that this methodology relies on the assumptions of the two-fluid model itself; it is then also very relevant to pursue research on the quality of models in this family to provide an accurate description of the problem, including for instance, relevant predictions of radial void fraction profiles and the effect of pressure imbalance. Advanced closures including pressure imbalance, surface-tension-induced pressure $\overline{p_l^b}^l$ and mixture momentum $\mathbf{M_m}$ will modify the system solution; it will in turn affect the construction of the macroscopic model and its closure relations. However, the extent of the changes and the conditions in which they are significant are unknown. It is important to keep in mind

that a more realistic pressure gradient (for instance by means of algebraic closures for local pressure differences as initiated in du Cluzeau et al. [36] and du Cluzeau et al. [48]) along with the consideration of the mixture momentum $\mathbf{M_m}$ have the potential to create additional diffusion in the macroscopic mixture model.

7. Insights into future applications

This section highlights the potentialities offered by the derivation presented in this article. It presents some guidelines to extract information from the rigorous open equation system for the local drift-flux or the macroscopic models (equation systems (35) or (49) respectively) from the content of finer solutions taken as references.

7.1. Applications to local modelling (two-fluid or drift-flux models)

As mentioned in section 4.5, the local resolution of the equation system for the couple $(\overline{\mathbf{u}}_m, \overline{\mathbf{u}}_r)$ is theoretically equivalent to that of the equation system for the couple $(\overline{\mathbf{u}}_l^l, \overline{\mathbf{u}}_v^v)$. However, in practice, choosing the couple $(\overline{\mathbf{u}}_m, \overline{\mathbf{u}}_r)$ can provide different numerical strategies to improve the stability of the numerical system and facilitate its resolution, with an improved robustness. Equation (16) governing the local relative velocity $\overline{\mathbf{u}}_r$ can be used directly in the implementation of the two-fluid model (coupled with equation (35c) that control the evolution of the mixture velocity $\overline{\mathbf{u}}_m$). This formulation is sometimes advantageous over the classical $(\overline{\mathbf{u}}_l^l, \overline{\mathbf{u}}_v^v)$ resolution because the coupling between phases through the interfacial transfers can be implicited more efficiently as it appears in a single equation.

But alternately, one could also consider partial simplifications of equation (16) to include only the dominant processes in the transport equation so as to achieve simpler models which could benefit from a simpler resolution and yet be capable of incorporating selected effects as transient convection or lift-induced migration for instance. This option would provide an alternate path between the local two-fluid model and a local drift flux model.

Lastly, if the relative velocity $\overline{\mathbf{u}}_r$ is fully reduced to a local instantaneous algebraic equation, a local equivalent to the homogenised drift-flux model can be obtained for fully three-dimensional cases. This local constitutive relation should incorporate the effect of interfacial forces. Provided that relevant closure relations can be found for specific configurations, the application of this strategy could be an interesting prospect for industrial studies in

which the knowledge of the local distribution is important, yet the direct use of the two-fluid model is too complicated. For instance, the prediction of the CHF occurrence could be improved by this kind of local model by detaching the modelling of the triggering mechanism from the consideration of a specific geometry. All these intermediate local models can be assessed on experimental data, but also on fully numerical procedures when considering the two-fluid model as a (richer, hence more accurate) reference.

Local relative velocity. From the local relative velocity obtained numerically (either by the complete two-fluid model or by any simplification of it) in various configurations, new constitutive relations can be inferred. From CMFD simulations resolving the two-fluid model, for various geometries and varying the fluid properties and/or the flow conditions, one can assess the contributions to equation (16) to determine the dominant effects and evaluate the appropriateness of the proposed closure relations for these mechanisms. Generally, interfacial transfers are considered as the predominant phenomena, but equation (16) reveals that other contributions are poorly known and may not be neglected based on *a priori* principles: *e. g.,* surface tension effects ($\mathbf{M_m}$) and their consequences on pressure gradients (especially in the cross-flow direction, ∇p_m and $\nabla\left(\alpha_v \overline{p}_r + \overline{p_l^b}^l\right)$), or liquid and vapour turbulent stresses ($\mathcal{T}_l^t$ and $\mathcal{T}_v^t$). This kind of evaluation will provide valuable information to connect the drift-flux model to the two-fluid model and assess its limits; it may potentially offer alternative strategies to alleviate some of them.

7.2. Applications to macroscopic modelling (space-averaged)

By construction, macroscopic models depend on the geometry considered; they are applicable only for a given geometry; corrections or extrapolations are required to apply them to new geometries. For the sake of the discussion, we will consider the geometry of a thin rectangular channel homogenised over the direction of the small gap e, but the discussion could be similarly transposed to a sub-channel in a rod-bundle or any representative configuration of a porous media (usually called *Representative Elementary Volume, REV* or averaging control volume). For this example, the geometry is illustrated on figure 3. Space-averaging is performed on the y-direction such that the macroscopic problem is bidimensional in the (x, z) plane.

The general procedure goes as follows:

- Define a geometry and the associated control volume or REV.

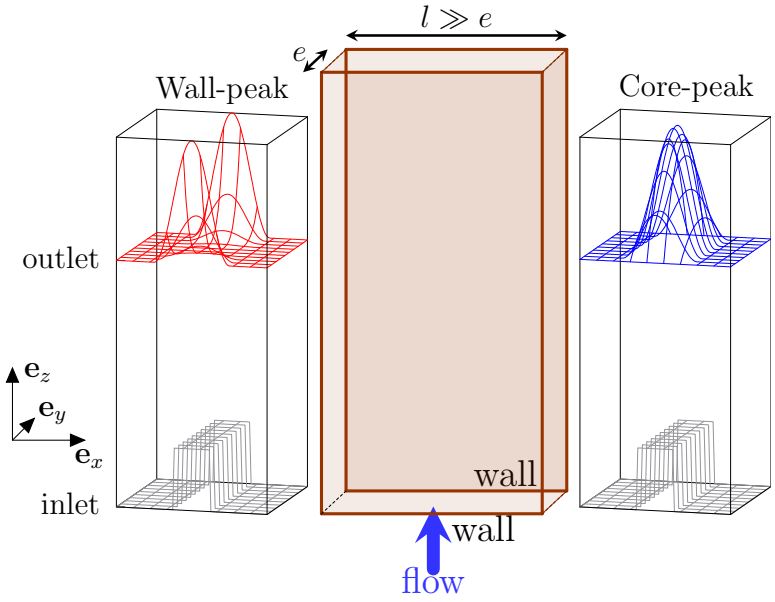

Figure 3: Schematic illustration of a thin rectangular channel considered for a homogenised description along y-axis. Vapour is uniformly injected at the centre of the channel and it can transition either to a wall-peaked flow (red, left curve) or to a core-peaked flow (blue, right curve).

- Select the mechanism $\mathcal{M}$ to model. Make it dimensionless based on macroscopic or global variables.

- Determine dimensionless parameters $\mathcal{N}_i$ and the macroscopic variables that are relevant to describe the evolution of the mechanism. They should depend only on the global conditions or on the macroscopic solution; they are considered as known in *a priori* tests. They cannot be related to local (microscopic) fields as they will intervene in the final model closure.

- Define several set of conditions to cover the dimensionless space.

- Force or ensure flow conditions that trigger the model.

- Perform reference simulations with the fine scale model (two-fluid or local drift-flux) for each condition.

- Average and post-process the solution field in each condition to determine reference values for the model $\mathcal{M}^{\text{ref}}(\mathcal{N}_0, \ldots, \mathcal{N}_i)$ and the macroscopic solution fields.

- Depending on the *a priori* knowledge of the mechanisms, two options are possible:

  If the actual form of the correlation is determined by theoretical considerations, a simple fitting of coefficients can be performed to minimise the difference $\epsilon = |\mathcal{M}^{\text{ref}} - \mathcal{M}^{\text{mod}}|$ over the sets of conditions simulated.

  If the form of the closure relation is unknown, variable selection and regression should be performed, either by classical approaches or by machine learning techniques (Support Vector Machine, ...).

In the following, two mechanisms are described to illustrate concretely the up-scaling methodology proposed.

Void fraction distribution. As an illustrative example, we consider the distribution of void fraction in the channel. Figure 3 sketches two characteristic behaviours that the diffusion of void fraction may generate (wall or core-peak). From a modelling point-of-view, it is then important to model diffusion of void fraction in equation (49b) due to the mechanism $\mathcal{M}_{\text{disp}} = \nabla_\phi \cdot (\rho_M \overline{\mathbf{u}}_D)$, in the cross-flow direction x. In many configurations, due to global variations

of the macroscopic solution (flow asymmetry, flow reduction due to corner effect) some effects of the local void fraction distribution or of the velocity gradients remain important at the macroscopic scale. For instance, powered by the local lift force, these gradients will be responsible for global migration of the vapour and macroscopic transverse velocity.

Concerning the distribution of void in the channel, a methodology similar to Zuber and Findlay [22] can be applied; however, our proposal is to produce numerically informed data by an appropriate selection of local two-fluid simulations in order to provide numerical values of the form

$$\mathcal{M}_{\text{disp}}^{\text{ref}} = \mathcal{M}_{\text{disp}}^{\text{ref}}\left(\text{Re}_M, c_M, d_b/e, \dots\right) \tag{56}$$

where $\text{Re}_M = \rho_M \left\|\overline{\mathbf{u}}_M\right\| D_h/\mu^\star$ is the macroscopic Reynolds number, D_h the hydraulic diameter and $\mu^\star$ some selected combination of liquid and vapour viscosities.

To derive a model $\mathcal{M}_{\text{disp}}^{\text{mod}}$ for this specific mechanism, one can for instance, compute from the local solution of CMFD simulations the distribution coefficient C_0 and the drift-velocity V_{Gj} as defined by Zuber and Findlay [22]. Finally, from this approach, it should be possible to extend the original work of Zuber and Findlay [22] to 3D applications, and from there, calibrate for instance the tensorial coefficients $\mathcal{C}_0$ proposed by Grégoire and Martin [21], in order to recover in the end an approximate expression $\mathcal{M}_{\text{disp}}^{\text{mod}}$ to model the void fraction dispersion based on macroscopic variables only.

Equation (50) reveals that all the components of the macroscopic drift velocity $\overline{\mathbf{u}}_D$ can be determined from the knowledge of microscopic (local) fields. Our intent in the future is to use this expression and to evaluate it on representative two-fluid simulations in order to provide the information necessary to accurately close the drift contribution in the divergence in equation (49b). This macroscopic mechanism is essential to appropriately describe the macroscopic migration of void fraction in the cross-flow direction. This lateral migration is then essentially due to sub-filter variations of the variables' profiles (velocity and void fraction mostly), and it depicts a mechanism fundamentally different from the original concept by Zuber and Findlay [22] that was dedicated to gravitational effects.

Macroscopic pressure drop. Another example where the effect of the underlying flow profile must be modelled is the prediction of the pressure drop along the flow. Equation (49c) shows that the local profiles of both velocity and pressure contribute to the pressure loss. Then, post-processing local

simulations provides a way to assess the two contributions to the reference macroscopic source $\mathcal{M}_{\rm pd}^{\rm ref}$ responsible for the pressure drop, defined as:

$$\mathcal{M}_{\rm pd}^{\rm ref} = \langle \delta_s p_m \ \delta_w \mathbf{n} \rangle_f + \langle \mathcal{T}^v \ \delta_w \mathbf{n} \rangle_f \tag{57}$$

From these *numerical measurements*, an additional closure relation to impose a wall friction coefficient $C_{\rm pd}$ could be derived under the form

$$\mathcal{M}_{\rm pd}^{\rm mod} = C_{\rm pd} \left({\rm Re}_M, c_M, d_b/e, \dots \right) \rho_M \left\| \overline{\mathbf{u}}_M \right\| \overline{\mathbf{u}}_M \tag{58}$$

where the functional dependency of $C_{\rm pd}$ to dimensionless parameters has to be determined.[2]

From the knowledge of both $\mathcal{M}_{\rm pd}^{\rm ref}$, ρ_M and $\overline{\mathbf{u}}_M$ by the averaging of local solutions, one can propose and assess a formulation for the coefficient $C_{\rm pd}$ that minimises the error $\epsilon_{\rm pd} = \left| \mathcal{M}_{\rm pd}^{\rm ref} - \mathcal{M}_{\rm pd}^{\rm mod} \right|$.

The contributions to $\mathcal{M}_{\rm pd}^{\rm ref}$ defined from local quantities will be very sensitive to the flow regime because of the strong coupling between the microscopic phase distribution and the profiles of velocities. In particular, when the conditions are varied, the flow can experience a transition of the void fraction profile. In the case of bubbly flows, it has been observed experimentally [51, 52] that the interfacial forces acting on the bubbles drive them towards or away from the wall, resulting in wall-peaked or core-peaked void fraction profiles depending on the flow conditions. This transition in void fraction profiles has a dramatic effect on averaged flow quantities such as the wall shear stress, velocity profiles and turbulence levels.

For industrial applications, it is important to be able to quantify the impact of this wall- to core-peak transition (and the conditions in which it occurs) and to incorporate this information into macroscopic models. The variations of wall shear stress induced by this transition can be responsible for large scale flow redistribution that should be accurately captured by component-scale simulations. The proposed up-scaling approach should help to determine mechanistic models (because more information is available from simulations than from experimental measurements) that could replace the use of flow-regime maps and henceforth, extend the prediction capabilities with better confidence.

[2]For completeness, we mention that $C_{\rm pd}$ might be represented by a matrix to account for the strong anisotropy of the flow.

In conjunction with this numerical approach, our team is designing an experiment to produce CFD-grade reference data to support our numerical simulations and enable the global validation of the procedure. In this experiment, the adiabatic air-water flow in a thin rectangular channel will be analysed for various flow rates of each phase in vertical or inclined flow direction. We target local measurements of void fraction, bubble-sizes distributions, mean liquid and gas velocities, velocity fluctuations in the liquid. The measurements' resolution should be sufficient to capture the predominant variations and validate the numerical procedure.

8. Conclusion and prospects

This article presents a theoretical derivation of a homogenised model for turbulent two-phase flows. Turbulent fluctuations and phase intermittency are crucial mechanisms incorporated into the model considered. Application of the space-averaging technique is not limited to porous media. In fact, one industrial use of this work consists in applying this methodology to propose a one- or two-dimensional description of pipe flows or of turbulent two-phase flows in rectangular channels or tube bundles. There, the model acts to represent the effect of high-shear regions developing at the walls.

This macroscopic model describes the evolution of mixture variables, but includes the effects of both sub-filter spatial variations, turbulence, and local non-equilibrium in velocity, pressure and enthalpy. It is derived theoretically based on the local instantaneous Navier-Stokes equations. Several steps are involved in order to obtain the final macroscopic mixture model. The approach is based on a two-step up-scaling strategy. First, we recall the basic principles that constitutes the basis of the widely-used Euler-Euler two-fluid model. A discussion on the importance of models for the interfacial transfers and of the closure of the pressure has been included to demonstrate that assumptions on the local pressure imbalance and on surface tension effects will have consequences on the macroscopic model. Then, we proceed to a reduction of the local two-fluid model which relies on the algebraic closure of the relative velocity to enable the resolution of a system composed of mixture variables (density, velocity and enthalpy). A simpler local drift-flux model is then obtained. Finally, the second part of the up-scaling is applied to derive a macroscopic mixture model similar to the sub-channel models in use in the nuclear or oil and gas industries. This step resorts to a spatial average that

is commonly used in porous media applications. Here, it is used to eliminate the costly need to resolve boundary layers in internal flows.

At the end of this two-step up-scaling strategy, the model remains open, but we have fully described the theoretical content of the macroscopic models. This formulation governing the macroscopic evolution of the mixture can be compared to models used in practical applications (i) to better identify the origins of the models involved and (ii) to provide an alternative to progress in the models' development or in the calibration of closure laws.

Many prospects in terms of validation and models' development based on this up-scaling methodology are now open. They include the use of these expressions involving fine-scale flow description to propose and assess new formulations of models based on *a priori* analyses of local two-fluid simulations. In section 7, we illustrated that if the equation for the local relative velocity $\overline{\mathbf{u}}_r$ is simplified to keep only the dominant mechanisms, new opportunities may be taken to solve intermediate models (in between the local two-fluid model and a local drift-flux model) that are still local and account for unsteadiness and convective effects. Further reduction given by an algebraic closure for the local relative velocity demonstrates the various degrees of simplifications that can be applied to connect the two-fluid and the drift-flux models at the local scale. Series of such "numerical experiments" can be performed to efficiently cover the parametric space (including experimentally-challenging industrial conditions such as for instance high-pressure flows), and to test different kinds of local closures. Reference values for the models can be post-processed from these simulations in order to assess the dependency to dimensionless parameters and to calibrate parameters *a priori*. These closures based on two-fluid CMFD simulations, include the models' formulation and the calibration of closure relations.

Further prospects include the assessment of models' simplifications at different steps of the process. For instance, various kinds of two-fluid models can be compared to investigate hypotheses concerning interfacial transfer closures, or the effect of pressure imbalance, or the potential effect of surface tension. Also, the assessment of the simplifications necessary to the derivation of an algebraic closure for the relative velocity is an important feature that can be analysed. Predictions of the relative velocity should include components orthogonal to gravity (where buoyancy and drag are predominant); indeed, complex (and partially understood) phenomenon such as lift, laminar and turbulent dispersions or wall effects, are important mechanisms responsible for an effective diffusion of void fraction. They are intrinsically related

to the structure of local velocity fluctuations, to pressure disturbance by the walls and the inclusions, and to the phase intermittency.

Most discussions in this article were focused on the momentum equations and the relative motion between phases. As stated by Ishii and Hibiki [2, pp. 365-366], modelling the mixture thermal energy in the context of the drift-flux model is a considerable challenge. Future prospects could expand the discussion at the end of section 5 to analyse the benefits of different choices (mixture enthalpy and a closure relation for the thermal state between the two-phase or separate conservation equations). The additional effect of spatial average on the energy transfers is also in a very preliminary state in the literature.

Application of this new methodology to derive industrial models for multiphase flows of increasing complexity is expected to provide a new way to access information that would be difficult to obtain experimentally. Therefore, we plan to use this approach to assess and eventually revise closures used in industrial codes based on the recently acquired capabilities of CMFD. In section 7, we illustrated the principles of the up-scaling methodology proposed on two mechanisms: the void fraction dispersion and the macroscopic pressure drop.

9. Acknowledgement

The author is grateful to his colleagues and in particular Dr. du Cluzeau, François and Bergeron for fruitful discussions and for their careful proofreading of a previous version of this article.

References

[1] D. A. Drew, S. L. Passman, Theory of Multicomponent Fluids, springer ed., Springer, 1999. doi:10.1007/b97678.

[2] M. Ishii, T. Hibiki, Thermo-fluid dynamics of two-phase flow, springer ed., Springer, 2015. doi:10.1007/978-0-387-29187-1.

[3] C. Morel, Mathematical Modeling of Two-Phase Flow, Springer, 2015.

[4] M. Ishii, N. Zuber, Drag coefficient and relative velocity in bubbly, droplet or particulate flows, AIChE J. 25 (1979) 843–855. doi:10.1002/aic.690250513.

[5] Y. Liu, J. Talley, K. Hogan, J. Buchanan, A generic framework for multi-field two-phase flow based on the two-fluid model, Progress in Nuclear Energy 94 (2017) 80–92. URL: https://www.sciencedirect.com/science/article/pii/S0149197016301901. doi:https://doi.org/10.1016/j.pnucene.2016.08.011.

[6] S. Whitaker, Theory and applications of transport in porous media: the method of volume averaging, Kluwer Academic Publishers, 1999.

[7] A. S. Jackson, C. T. Miller, W. G. Gray, Thermodynamically constrained averaging theory approach for modeling flow and transport phenomena in porous medium systems: 6. two-fluid-phase flow, Advances in Water Resources 32 (2009) 779 – 795. URL: http://www.sciencedirect.com/science/article/pii/S0309170808002157. doi:https://doi.org/10.1016/j.advwatres.2008.11.010.

[8] F. J. Carrillo, I. C. Bourg, C. Soulaine, Multiphase flow modeling in multiscale porous media: An open-source micro-continuum approach, Journal of Computational Physics: X 8 (2020) 100073. URL: http://www.sciencedirect.com/science/article/pii/S2590055220300251. doi:https://doi.org/10.1016/j.jcpx.2020.100073.

[9] C. Soulaine, M. Quintard, On the use of a darcy-forchheimer like model for a macro-scale description of turbulence in porous media and its application to structured packings, International Journal of Heat and Mass Transfer 74 (2014) 88 – 100. URL: http://www.sciencedirect.com/science/article/pii/S0017931014001975. doi:https://doi.org/10.1016/j.ijheatmasstransfer.2014.02.069.

[10] W. G. Gray, A. F. Tompson, W. E. Soll, Closure conditions for two-fluid flow in porous media, Transport in Porous Media (2002). URL: https://doi.org/10.1023/A:1015035214629. doi:10.1023/A:1015035214629.

[11] G. Wallis, One-Dimensional Two-Phase Flow, mcgraw hill ed., Springer-Verlag, 1969.

[12] J. Delhaye, J. Achard, On the averaging operators introduced in two-phase flow modeling, Centre d'études nucléaires de Grenoble, 1976.

[13] J.-M. Delhaye, M. Giot, M. Riethmuller, Thermohydraulics of two-phase systems for industrial design and nuclear engineering, Hemisphere Publishing Corporation, 1980.

[14] J.-M. Delhaye, M. Giot, M. L. Riethmuller, Thermohydraulics of two-phase systems for industrial design and nuclear engineering, Hemisphere Publishing Corporation, 1981.

[15] J.-M. Delhaye, J.-G. Collier, G. Hewitt, A. E. Bergles, Two-phase flow and heat transfer in the process and power industries, Hemisphere Publishing Corporation, 1981. McGraw-Hill, New York.

[16] G. Yeoh, J. Tu, Basic Theory and Conceptual Framework of Multiphase Flows, 2016, pp. 1–47. doi:10.1007/978-981-4585-86-6_1-1.

[17] M. Ishii, T. Hibiki, Thermo-fluid dynamics of two-phase flow, springer, new york ed., Springer, 2006.

[18] N. Zuber, On the dispersed two-phase flow in the laminar flow regime, Chem. Eng. Sci. 19 (1964) 897–917. URL: http://www.sciencedirect.com/science/article/pii/0009250964850673. doi:10.1016/0009-2509(64)85067-3.

[19] S. Rassame, T. Hibiki, Drift-flux correlation for gas-liquid two-phase flow in a horizontal pipe, International Journal of Heat and Fluid Flow 69 (2018) 33–42. URL: https://www.sciencedirect.com/science/article/pii/S0142727X17307865. doi:https://doi.org/10.1016/j.ijheatfluidflow.2017.11.002.

[20] T. Hibiki, M. Ishii, One-dimensional drift-flux model and constitutive equations for relative motion between phases in various two-phase flow regimes, International Journal of Heat and Mass Transfer 46 (2003) 4935–4948. URL: https://www.sciencedirect.com/science/article/pii/S0017931003003223. doi:https://doi.org/10.1016/S0017-9310(03)00322-3.

[21] O. Grégoire, M. Martin, Derivation of a well-posed and multidimensional drift-flux model for boiling flows, Comptes Rendus Mécanique 333 (2005) 459–466.

[22] N. Zuber, J. Findlay, Average volumetric concentration in two-phase flow systems, Journal of Heat Transfer 87 (1965) 453–468.

[23] A. Nakayama, F. Kuwahara, A macroscopic turbulence model for flow in a porous medium, Journal of Fluids Engeneering 121 (1999) 427–433.

[24] A. Nakayama, F. Kuwahara, Y. Kodama, An equation for thermal dispersion flux transport and its mathematical modelling for heat and fluid flow in a porous medium, Journal of Fluid Mechanics 563 (2006) 81–96.

[25] M. H. J. Pedras, M. J. S. de Lemos, On the definition of turbulent kinetic energy for flow in porous media, International Communication in Heat and Mass Transfer 27 (2000) 211–220.

[26] M. H. J. Pedras, M. J. S. D. Lemos, Macroscopic turbulence modeling for incompressible flow through undeformable porous media, International Journal of Heat and Mass Transfer 44 (2001) 1081–1093.

[27] F. Pinson, Modélisation de l'échelle macrascopique d'un écoulement turbulent au sein d'un milieu poreux, Ph.D. thesis, Institut National Polytechnique de Toulouse, 2006.

[28] M. Drouin, Modélisation des écoulements turbulents anisothermes en milieu macroporeux par une approche de double filtrage, Ph.D. thesis, Institut National Polytechnique de Toulouse, 2010.

[29] M. Drouin, O. Grégoire, O. Simonin, A consistent methodology for the derivation and calibration of a macroscopic turbulence model for flows in porous media, International Journal of Heat and Mass Transfer 63 (2013) 401 – 413. URL: http://www.sciencedirect.com/science/article/pii/S0017931013002676. doi:https://doi.org/10.1016/j.ijheatmasstransfer.2013.03.060.

[30] O. Grégoire, M. Drouin, O. Simonin, Connecting dispersion models and wall temperature prediction for laminar and turbulent flows in channels, International Journal of Heat and Mass Transfer 55 (2012) 3100 – 3113. URL: http://www.sciencedirect.com/science/article/pii/S0017931012000749. doi:https://doi.org/10.1016/j.ijheatmasstransfer.2012.02.011.

[31] M. Chandesris, Modélisation des écoulements turbulents dans les milieux poreux à l'interface avec un milieu libre, Ph.D. thesis, Université de Paris 6, 2006.

[32] M. Chandesris, G. Serre, P. Sagaut, A macroscopic turbulence model for flow in porous media suited for channel, pipe and rod bundle flows, International Journal of Heat and Mass Transfer 49 (2006) 2739–2750.

[33] M. Chandesris, D. Jamet, Boundary conditions at a fluid-porous interface: An a priori estimation of the stress jump coefficients, International Journal of Heat and Mass Transfer 50 (2007) 3422 – 3436. URL: http://www.sciencedirect.com/science/article/pii/S0017931007001536. doi:https://doi.org/10.1016/j.ijheatmasstransfer.2007.01.053.

[34] R. Clavier, N. Chikhi, F. Fichot, M. Quintard, Modeling of inertial multi-phase flows through high permeability porous media: Friction closure laws, International Journal of Multiphase Flow 91 (2017) 243 – 261. URL: http://www.sciencedirect.com/science/article/pii/S030193221630235X. doi:https://doi.org/10.1016/j.ijmultiphaseflow.2017.02.003.

[35] W. Wang, B. Lu, J. Geng, F. Li, Mesoscale drag modeling: a critical review, Current Opinion in Chemical Engineering 29 (2020) 96 – 103. URL: http://www.sciencedirect.com/science/article/pii/S2211339820300447. doi:https://doi.org/10.1016/j.coche.2020.07.001.

[36] A. du Cluzeau, G. Bois, A. Toutant, J.-M. Martinez, On bubble forces in turbulent channel flows from direct numerical simulations, J. Fluid Mech. 882 (2020) A27. doi:10.1017/jfm.2019.207.

[37] I. Kataoka, Local instant formulation of two-phase flow, Int. J. Multiph. Flow 12 (1986) 745–758. doi:10.1016/0301-9322(86)90049-2.

[38] G. Tryggvason, B. Bunner, A. Esmaeeli, N. Al-Rawahi, Computations of Multiphase Flows, Adv. Appl. Mech. 39 (2003) 81–120. doi:10.1016/S0065-2156(02)39002-1.

[39] J. Delhaye, Equations Fondamentales des écoulements diphasiques, Part 1 and 2, Technical Report CEA-R-3429, CEA, 1968.

[40] J.-M. Delhaye, Jump conditions and entropy sources in two-phase systems. Local instant formulation, International Journal of Multiphase Flow 1 (1974) 395–409.

[41] J.-M. Delhaye, Thermohydraulique des réacteurs, adp sciences ed., ADP sciences, 2008.

[42] G. Bois, Transferts de masse et d'énergie aux interfaces liquide / vapeur avec changement de phase : proposition de modélisation aux grandes échelles des interfaces, Ph.D. thesis, Université de Grenoble, 2011. URL: http://tel.archives-ouvertes.fr/tel-00627370.

[43] N. Panicker, A. Passalacqua, R. Fox, On the hyperbolicity of the two-fluid model for gas–liquid bubbly flows, Applied Mathematical Modelling 57 (2018) 432 – 447. URL: http://www.sciencedirect.com/science/article/pii/S0307904X18300234. doi:https://doi.org/10.1016/j.apm.2018.01.011.

[44] S. P. Antal, R. T. Lahey, J. E. Flaherty, Analysis of phase distribution in fully developed laminar bubbly two-phase flow, Int. J. Multiph. Flow 17 (1991) 635–652. doi:10.1016/0301-9322(91)90029-3.

[45] N. Lubchenko, B. Magolan, R. Sugrue, E. Baglietto, A More Fundamental Wall Lubrication Force from Turbulent Dispersion Regularization for Multiphase CFD Applications, Int. J. Multiph. Flow 98 (2017) 36–44. URL: http://dx.doi.org/10.1016/j.ijmultiphaseflow.2017.09.003. doi:10.1016/j.ijmultiphaseflow.2017.09.003.

[46] S. Mimouni, M. Guingo, J. Lavieville, N. Mérigoux, Combined evaluation of bubble dynamics, polydispersion model and turbulence modeling for adiabatic two-phase flow, Nucl. Eng. Des. 321 (2017) 57–68. doi:10.1016/j.nucengdes.2017.03.041.

[47] Neptune_CFD Development Team, Neptune_CFD version 6.0.0 Theory Guide, Technical Report 6125-3013-2019-03351-FR, EDF R&D – CEA, 2019.

[48] A. du Cluzeau, G. Bois, A. Toutant, Modelling of the laminar dispersion force in bubbly flows from direct numerical simulations, Physics of Fluids 32 (2020) 012106. URL:

https://doi.org/10.1063/1.5132607. doi:10.1063/1.5132607. arXiv:https://doi.org/10.1063/1.5132607.

[49] S. Whitaker, Diffusion and dispersion in porous media, AIChE 3(13) (1967) 420–427.

[50] F. A. Howes, S. Whitaker, The spatial averaging theorem revisited, Chemical Engineering Science 40 (1985) 1387–1392.

[51] A. Tomiyama, H. Tamai, I. Zun, S. Hosokawa, Transverse migration of single bubbles in simple shear flows, Chem. Eng. Sci. 57 (2002) 1849–1858. doi:10.1016/S0009-2509(02)00085-4.

[52] T. Hibiki, M. Ishii, Experimental study on interfacial area transport in bubbly two-phase flows, International Journal of Heat and Mass Transfer 42 (1999) 3019–3035.

Declaration of interests

☒The authors declare that they have no known competing financial interests or personal relationships that could have appeared to influence the work reported in this paper.

☐The authors declare the following financial interests/personal relationships which may be considered as potential competing interests:

Declaration of interests

☒The authors declare that they have no known competing financial interests or personal relationships that could have appeared to influence the work reported in this paper.

☐The authors declare the following financial interests/personal relationships which may be considered as potential competing interests: